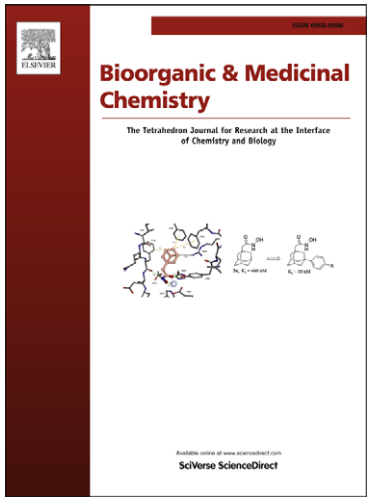


# Novel 1,3,4-Oxadiazole Thioether Derivatives Targeting Thymidylate Synthase as Dual Anticancer/Antimicrobial Agents

Qian-Ru Du, Dong-Dong Li, Ya-Zhou Pi, Jing-Ran Li, Jian Sun, Fei Fang, Hai-Bin Gong, Hai-Liang Zhu

PII: S0968-0896(13)00132-6
DOI: http://dx.doi.org/10.1016/j.bmc.2013.02.008
Reference: BMC 10603

To appear in: *Bioorganic & Medicinal Chemistry*

Please cite this article as: Du, Q-R., Li, D-D., Pi, Y-Z., Li, J-R., Sun, J., Fang, F., Gong, H-B., Zhu, H-L., Novel 1,3,4-Oxadiazole Thioether Derivatives Targeting Thymidylate Synthase as Dual Anticancer/Antimicrobial Agents, *Bioorganic & Medicinal Chemistry* (2013), doi: http://dx.doi.org/10.1016/j.bmc.2013.02.008

# Novel 1,3,4-Oxadiazole Thioether Derivatives Targeting Thymidylate Synthase as Dual Anticancer/Antimicrobial Agents

*Qian-Ru Du* [a+], *Dong-Dong Li* [a+], *Ya-Zhou Pi* [a], *Jing-Ran Li* [a], *Jian Sun* [a], *Fei Fang* [a], *Hai-Bin Gong* [b*], *Hai-Liang Zhu* [a*]

[a] *State Key Laboratory of Pharmaceutical Biotechnology, Nanjing University, Nanjing 210093, P. R. China.*

[b] *Xuzhou Central Hospital, Xuzhou 221009, P. R. China.*

[+] These authors contributed equally to this work.

* Corresponding authors. Tel./fax: +86-25-83592672;

*E-mail address*: zhuhl@nju.edu.cn

**Abstract:** A series of novel 1,3,4-oxadiazole thioether derivatives (compounds **9-44**) were designed and synthesized as potential inhibitors of thymidylate synthase (TS) and as anticancer agents. The *in vitro* anticancer activities of these compounds were evaluated against three cancer cell lines by the MTT method. Among all the designed compounds, compound **18** bearing a nitro substituent exhibited more potent in vitro anticancer activities with $IC_{50}$ values of 0.7 ± 0.2 $\mu$M, 30.0 ± 1.2 $\mu$M, 18.3 ± 1.4 $\mu$M, respectively, which was superior to the positive control. In the further study, it was identified as the most potent inhibitor against two kinds of TS protein (for human TS and *E. coli* TS, $IC_{50}$ values: 0.62 $\mu$M and 0.47 $\mu$M, respectively) in the TS inhibition assay *in vitro* and the most potent antibacterial agents with MIC (minimum inhibitory concentrations) of 1.56-3.13 $\mu$g/mL against the tested four bacterial strains. Molecular docking and 3D-QSAR study supported that compound **18** can be selected as dual antitumor/antibacterial candidate in the future study.

**Keywords:** Thymidylate Synthase; 1,3,4-Oxadiazoles; Metronidazole; X-ray crystallography; Anticancer activities

## 1. Introduction

Thymidylate synthase (TS) has long been recognized as an important and attractive target for chemotherapy because of its vital role in DNA biosynthesis.[1] It catalyzes the reductive methylation of 2'-deoxyuridine 5'-monophosphate (dUMP) to 2'-deoxythymidine 5'-monophosphate (dTMP), which could be converted to a triphosphate (dTTP) by deoxyribonucleoside diphosphate kinase and subsequently be incorporated into DNA. This reaction provides a sole de novo pathway for the production of dTMP and the oxidization of 5,10-methylenetetrahydrofolate during one-carbon transfer.[2] TS inhibition, which leads to deoxynucleotide (dNTP) pool imbalances, is an attractive strategy for the development of antitumor agents.[3] In the early 1950s, 5-fluorouracil (5-FU) as a pyrimidine analog which works through irreversible inhibition of TS, was a prominent antitumor agent. The emergence of resistance as well as the insensitivity of certain tumor types to 5-FU has triggered the design of novel folate analogs as potential TS inhibitors and anticancer agents.[4] Several compounds with dual inhibitory activity of TS and dihydrofolate reductase (DHFR) in **Figure 1**, such as Raltitrexed (ZD1694) and Pemetrexed (LY231514) , have been approved as antitumor agents[5-6]. These drugs that possess a benzoyl L-glutamic acid side chain similar to natural folates could be polyglutamated by folyl polyglutamate synthetase (FPGS) [7] to the pentaglutamate forms which could be easily transferred into cells, leading to high intracellular concentrations of these antitumor agents. Although polyglutamylation can increase potent inhibitory activity, it is also involved with the toxicity in host cells and can not circumvent tumors with low levels of FPGS.[8] Facing the problems associated with classical antifolates, several strategies have been put forward, such as designing nonclassical lipophilic antifolate analogs that would not dependent on FPGS for their potency, or designing novel 5-FU analogs only targeting TS. As displayed in **Figure 2**, the first nonclassical TS inhibitor, AG337 (nolatrexed) has been studied under a series of clinical trials;[9] Gangjee *et al.* also designed several potent TS inhibitors (**1-3**) based on the X-ray crystal structure of

TS and AG337.[8,10-11] Although other important successful works have been completed in the field of nonclassical antifolate, TS will still present ample opportunities for scientists in drug discovery field .

**(Figure 1)**

**(Figure 2)**

1,3,4-Oxadiazoles possessing a variety of biological activities[12-15]which belongs to an important class of heterocyclic compounds. The widespread use of them as a scaffold in medicinal chemistry establishes this moiety as a member of the privileged structures class. In particular, a few of differently substituted 1,3,4-oxadiazoles have been found to exhibit anticancer activities.[16-17] Moreover, 1,3,4-oxadiazole heterocycles are very good bioisosteres of amides and esters, which contribute substantially to increasing pharmacological activity by participating in hydrogen bonding interactions with the receptors.[18] Nitroimidazoles are extensively used as antimicrobial chemotherapeutics and as antiangiogenic hypoxic cell radiosensitizers.[19] Their derivatives have attracted considerable attentions due to showing a tendency to penetrate and accumulate in regions of tumors[20-21] and can undergo bioreduction to yield electrophilic substances that can attack proteins and nucleic acids.[22] Importantly, the toxicology and metabolism of nitroimidazoles, particularly metronidazole, have been characterized.[23-24] Thus, nitroimidzaoles may provide an attractive possibility for employing these molecules as carriers to targeted delivery in cancer therapy.[25-26] Recently, Swenson *et al*. synthesized a $^{10}$B-enriched nitroimidazole by coupling the Cs salt of BSH ($Cs_2$-$^{10}B_{12}H_{11}SH$) with 1-(2-bromoethyl)-2-methyl-5-nitroimidazole and it was used for boron neutron capture therapy of cancer.[27]

Based on the statements above, a bold attempt to design a series of novel scaffold TS inhibitors by coupling 1,3,4-oxadiazole with metronidazole moiety has been put forward for the first time. **Figure 1** shows in detail the composition of these novel TS inhibitors, in which the metronidazole part seems like a warhead that

directs the whole molecule to the hypoxic tissue, such as the regions of solid tumors; while 1,3,4-oxadiazole part would presumably mimics 5-FU as a pharmacophore. In aim to investigate whether the designed compounds could work on TS protein, docking simulations were performed on the two known TS protein crystal structure (PDB code: 1HVY derived from human TS, and 2KCE derived from *E. coli* TS). The obtained results have been presented in **Figure 3**, describing the binding energy and CDOCKER_INTERACTION_ENERGY of all the designed compounds. Compared with the positive drug, AG337, most of the designed molecules below the blue dash lines possess lower binding energies and interaction energies, demonstrating these compounds are likely to exhibit more potent against both of the two protein targets. **Figure 3A** showed the binding energies of designed molecules interacting with two TS protein targets, among which two compounds **18**, **37** worked very well both in 2KCE and 1HVY proteins. **Figure 3B** also displayed the alternative measure of the protein-ligand interaction by CDOCKER-_INTERACTION_ENERGY which was used to accurately estimate the results of the docking study.[28] Taken together from the two pictures, compound **18** performed best in the two kinds of evaluation programs, in which its binding energy and docking energy could reached up to -92.5608, and -46.2693 kcal/mol, respectively. Therefore, these preliminary works would serve as a modest spur to induce us to probe these 1,3,4-oxadiazole scaffold compounds. In this manuscript, we described the synthesis and the structure activity relationships (SAR) of a series of novel 1,3,4-oxadiazole analogs as TS inhibitors and as dual antitumor/antimicrobial agents. Moreover, according to the binding model, we established a 3D-QSAR model to provide a marker post for the development of novel TS inhibitors based on the 1,3,4-oxadiazole scaffold.

**(Figure 3)**

## 2. Results and discussion

### 2.1. Chemistry

The key intermediates **6** were prepared in three steps by the procedure shown in **Scheme 1** [17]. Esterification of the carboxylic acids with the mixture of ethanol and concentrated sulfuric acid afforded the corresponding esters **4**. The aroyl hydrazides **5** were obtained by the reaction of esters **4** with 85% hydrazine hydrate in ethanol. Treatment of the hydrazides **5** with carbon disulfide in the presence of KOH in 95% ethanol under reflux gave the key intermediates **6**. 1-(2-Bromoethyl)-2-methyl-5-nitro-1*H*-imidazole **8** was synthesized from metronidazole by bromizing as previously described (**Scheme 2**)[29]. The synthesis of the target compounds **9-44** was accomplished by refluxing compounds **6** with 1-(2-bromoethyl)-2-methyl-5-nitro-1*H*-imidazole **8** in the presence of NaOEt in EtOH (**Scheme 3**). The resulting **9-44** are all new compounds.

**(Scheme 1)**

**(Scheme 2)**

**(Scheme 3)**

All of the synthetic compounds have presented both satisfactory analytical and spectroscopic data, which were in full accordance with their depicted structures. Additionally, the structure of compound **9** was further confirmed by X-ray diffraction and its crystal data was presented in **Table 1**. Besides, **Figure 4** gave a perspective view of this compound together with the atomic labeling system.

**(Table 1)**

**(Figure 4)**

**2.2. Bioassays and SAR**

All newly synthesized compounds **9-44** were evaluated for their *in vitro* anticancer activities against HepG2 (human hepatoma cells), SGC-7901 (human gastric cancer cells), and MCF-7 (human breast cancer cells) cell lines. The results were summarized in **Table 2**. A number of 1,3,4-oxadiazole thioether derivatives showed remarkable effects on anticancer activities. To our delight, all compounds **9-44** displayed potent inhibition activities against HepG2 cell lines. Among the compounds tested, compounds **11**, **17**, **18**, **21**, **40** exhibited potent inhibitory activities against HepG2 cell lines ($IC_{50}$ < 3 $\mu$M; as for **11**, $IC_{50}$ = 2.2 ± 0.2 $\mu$M; as for **17**, $IC_{50}$ = 1.9 ± 0.4 $\mu$M; as for **18**, $IC_{50}$ = 0.7 ± 0.2 $\mu$M; as for **21**, $IC_{50}$ = 0.6 ± 0.2 $\mu$M; as for **40**, $IC_{50}$ = 0.9 ± 0.3 $\mu$M), which were more potent than the positive control 5-fluorouracil (5-FU). Besides, it was worth mentioning that eight target compounds (**11, 13, 17, 19, 21, 31, 39 and 44**) showed potent anticancer activities against the other SGC-7901, and MCF-7 cell lines, all of which were more potent than the positive control 5-FU.

**(Table 2)**

Generally, structure-activity relationships (SAR) at the cellular level for these 1,3,4-oxadiazole thioether derivatives demonstrated that compounds with substituents at *para* position of benzene ring had a moderate increase of activity than those at *ortho* position, comparing compounds (**11**, **13**, **15**, **17**, **21**, **23**) to compounds (**10**, **12**, **14**, **16**, **20**, **22**), respectively. Unlike these compounds, compound **19** bearing a nitro substituent at *para* position of the phenyl ring was actually inferior to the corresponding compound **18** with nitro substituent located at *ortho* position of the phenyl ring, which indicated that nitro group at the proper position of the benzene ring may play an important role on the anticancer activities. Moreover, **Table 2** also listed other designed molecules in which the phenyl ring was replaced by five kinds of the heterocycles (furan: **33**; thiophene: **34**; pyridine: **35**-**41**; naphthalene: **42**, **43**; deoxygenated ring: **44**). In general, most compounds exhibited modest anti-proliferative activities against the three cancer cells except for **40,** and the

replacement of the pyridine ring was more likely to increase compounds' biological activity than those of other sorts of rings. On the other hand, electron withdrawing groups of the phenyl ring performed better than electron donating groups on anti-proliferative activity, no matter the replacement at *ortho* position or *para* position, and the similar influence was also observed on heterocycle substitution. Disubstituted or three substituted donating groups could provide a little effect on improving anti-proliferative activity when referring to **28**-**32**. However, compounds **32**, **37** were considered as the two best compounds in the analysis of the molecular docking study whereas they performed not well in the "wet experiment" above. In the next step, eleven compounds including **32** and **37**, would be selected and be further evaluated for the TS inhibition assay.

**(Table 3)**

**(Table 4)**

Compounds **11**, **17**, **18**, **21, 25, 26, 32, 37, 40, 41** and **44**, were evaluated as inhibitors of human TS and *Escherichia coli* TS (**Table 3**). All of the compounds were moderate to potent inhibitors of human TS, in which their $IC_{50}$ values were in the range of 0.62-3.9 $\mu$M against hTS. Compounds **18** and **40** were two most potent inhibitors of hTS and *E. coli* TS that comparable in potency to clinically used analog Raltitrexed (ZD1694). These two compounds (**18**, **40**) were approximately 15- and 10-fold more potent than Pemetrexed (LY231514), respectively. In addition, it was noticeable that although the two predicted potent inhibitors (**32**, **37**) showed better inhibitory activities in the TS assay *in vitro*, the possible explanation for the loss in potency of anticancer cells could be probably attributed to higher molecular weight (as to **32**, MW: 421.428) and lower ALOGP values (as to **37**, ALOGP: 0.886). As summarized in **Table 3**, compounds **18**, **40** possessed potent inhibitory activities against both hTS and *E. coli* TS, and subsequently would be picked up to test their relative antibacterial activity. Taken together, compounds (**18**, **37**, **40**) were evaluated

for antibacterial activity against two Gram-negative bacterial strains: *E. coli* and *P. fluorescence* and two Gram-positive bacterial strains: *B. subtilis* and *S. aureus* by the MTT method. **Table 4** presented in detail the antibacterial data of these dual functional agents. Compound **18** showed the most potent antibacterial activity with MIC (minimum inhibitory concentrations) of 1.56–3.13 $\mu$g/mL against the tested bacterial strains, comparable in potency to clinically known antibacterial agent kanamycin, and could be selected to improve as dual antitumor/antibacterial agent in the future study.

**(Figure 5)**

A docking study of the most active compound **18** and the two TS protein was performed to validate the structure-activity relationship (SAR) of similar compounds. As seen in **Figure 5**, the structures of **18** had been docked in the crystal structure of human TS and *E. coli* TS (PDB ID: 1HVY and 2KCE), respectively. Docking results (**Figure 5A** and **5C**) revealed that amino acid Asn 226 in the binding pocket of 1HVY protein and three amino acids Trp80, Trp83, His207 in the binding pocket of 2KCE protein played vital roles in the conformation of **18**, which were stabilized by *Pi-Cation* bond, *Pi-Pi* bond, and hydrogen bond that shown in 2D diagram. Besides, the lead compound was described to stretch up in the binding site to reduce the interaction energy.

In order to obtain a systematic SAR profile on 1,3,4-oxadiazole thioether analogs as antitumor agents and to explore the more potent and selective TS inhibitors, 3D-QSAR model was built using the corresponding $pIC_{50}$ values which were converted from the obtained $IC_{50}$ values ($\mu$M) of human TS inhibition (the way of this transformation was derived from an online calculator developed by an indian medicinal chemistry lab (http://www.sanjeevslab.org/tools-IC50.html) and performed by built-in QSAR software of DS 3.1 (Discovery Studio 3.1, Accelrys, Co. Ltd). The training and test sets were divided by the random diverse molecules method of DS 3.1, in which the training set accounted for 80% of all the molecules while the test set was

set to 20%. The training set was composed of 10 agents and the relative test set comprised 3 agents, which had been presented in **Table 5**. One key issue in the development of 3D-QSAR model was to determine the active conformation and how to align these molecules reasonably. An efficient solution in this study mainly depends on the docking study and the reliability of this method has been documented in previous studies.[30]

**(Table 5)**

In default situation, the alignment conformation of each molecule was the one that possessed the lowest CDOCKER_INTERACTION_ENENGY among the twenty docked poses. The 3D-QSAR model which generated from DS 3.1, defined the critical regions (steric or electrostatic) affecting the binding affinity. It was a PLS model built on 400 independent variables (conventional $R^2$= 0.87). The observed and predicted values and the corresponding residual values for the training set and test set molecules in 3D-QSAR model were listed in **Table 5**. Moreover, their graphical relationship was illustrated in **Figure 6A**, in which the plot of observed $IC_{50}$ versus the predicted results showed that this model could be used in prediction of activity for novel 1,3,4-oxadiazole thioether derivatives as TS inhibitors.

**(Figure 6)**

A contour plot of the electrostatic field region favorable (in blue) or unfavorable (red) for anticancer activity based on TS protein target were displayed in **Figure 6B** while the energy grids corresponding to the favorable (in green) or unfavorable (yellow) steric effects for the TS affinity were displayed in **Figure 6C**. It was widely acceptable that a better inhibitor based on the 3D QSAR model should have a strong Van der Waals attraction in the green areas and a polar group in the blue electrostatic potential areas (which were dominant close to the skeleton). As expected, those potent compounds (**11**, **17**, **18** and so on) not only could circumvent the red subregion or the

unfavorable yellow steric subregion but also can get more close to the favorable blue and green spaces. Thus, this promising model would provide a guideline to design and optimize more effective TS inhibitors and pave the way for us in the further study.

## 3. Conclusion

In summary, a series of novel 1,3,4-oxadiazole thioether derivatives based on 1-(2-hydroxyethyl)-2-methyl-5-nitroimidazole (metronidazole) scaffold have been synthesized and the cytotoxic activities of all the compounds were assessed against three cancer cell lines. The SAR for these designed compounds against human TS reveals that the sort and position of the substituent(s) on the phenyl ring or heterocycle are important. It can be simply concluded that the nature of the electron withdrawing group at 4'-position of the phenyl ring is detrimental to potent TS inhibition. In particular, compound **18** bearing nitro substituent exhibits more potent *in vitro* anticancer activities with $IC_{50}$ value of 0.7 ± 0.2 $\mu$M, 30.0 ± 1.2 $\mu$M, 18.3 ± 1.4 $\mu$M, respectively, which was superior to the positive control. In the further study, it can be identified as the most potent inhibitor against two kinds of TS proteins (as for hTS and *E. coli* TS, $IC_{50}$ values: 0.62 $\mu$M and 0.47$\mu$M, respectively) in the TS assay *in vitro* and the most potent antibacterial agent with MIC (minimum inhibitory concentrations) of 1.56-3.13 $\mu$g/mL against the tested four bacterial strains. Molecular docking and 3D-QSAR study support that compound **18** can be selected as dual antitumor/antibacterial candidate in the future study.

## 4. Experimental

### *4.1. Chemistry*

All chemicals and reagents used in current study were analytical grade. The reactions were monitored by the thin layer chromatography (TLC) on Merck pre-coated silica GF254 plates. Melting points (uncorrected) were determined on a XT4MP apparatus (Taike Corp., Beijing, China). ESI mass spectra were obtained on a Mariner System 5304 mass spectrometer, and $^1$H NMR spectra were collected on a

Bruker DPX500 or DPX300 spectrometer at room temperature with TMS and solvent signals allotted as internal standards. Chemical shifts were reported in ppm ($\delta$). Elemental analyses were performed on a CHN-O-Rapid instrument, and were within ±0.4% of the theoretical values.

*4.1.1. General procedure for the preparation of target compounds* ***9-44***

To a stirred solution of compound **6** (2 mmol) and sodium ethoxide (0.16 g, 2.4 mmol) in anhydrous ethanol (30 mL), 1-(2-bromoethyl)-2-methyl-5-nitro-1*H*-imidazole **8** (0.47 g, 2 mmol) was added. The resulting mixture was heated under reflux for 8-36 h, and the reaction was monitored by the thin layer chromatography (TLC). Afterwards the solution was cooled to room temperature and the organic solvent was removed *in vacuo*. The residue was dissolved in dichloromethane and the organic layer was washed with water and saturated brine, respectively. Then the organic phase was dried over anhydrous $Na_2SO_4$, filtered, and removed *in vacuo*. The purification of the residue by recrystallization from anhydrous ethanol afforded the desired compounds **9-44**.

*4.1.1.1.*

*2-((2-(2-methyl-5-nitro-1H-imidazol-1-yl)ethyl)thio)-5-phenyl-1,3,4-oxadiazole (**9**)*

Light brown powder, yield: 60.9%, mp: 119-120 □. $^1$H NMR (300 MHz, $CDCl_3$) $\delta$: 2.61 (s, 3H), 3.66 (t, $J$ = 6.9 Hz, 2H), 4.83 (t, $J$ = 6.9 Hz, 2H), 7.49-7.59 (m, 3H), 7.99-8.03 (m, 3H). $^{13}$C NMR (100 MHz, $CDCl_3$) $\delta$: 162.34, 159.39, 149.72, 139.65, 133.46, 131.57, 129.06, 127.08, 126.66, 42.18, 26.59, 16.82. MS (ESI): 332.1 ($C_{14}H_{14}N_5O_3S$, $[M+H]^+$). Anal. Calcd for $C_{14}H_{13}N_5O_3S$: C, 50.75; H, 3.95; N, 21.14; Found: C, 50.63; H, 3.96; N, 21.17.

*4.1.1.2.*

*2-((2-(2-methyl-5-nitro-1H-imidazol-1-yl)ethyl)thio)-5-(o-tolyl)-1,3,4-oxadiazole (**10**)*

Light yellow powder, yield: 65.6%, mp: 84-85 □. $^1$H NMR (500 MHz, $CDCl_3$) δ: 2.63 (s, 3H), 2.73 (s, 3H), 3.69 (t, $J$ = 6.8 Hz, 2H), 4.87 (t, $J$ = 6.8 Hz, 2H), 7.34-7.39

(m, 2H), 7.46 (t, $J$ = 7.5 Hz, 1H), 7.91 (d, $J$ = 7.5 Hz, 1H), 8.01 (s, 1H). $^{13}$C NMR (100 MHz, $CDCl_3$) $\delta$: 162.34, 149.72, 148.76, 139.65, 136.59, 133.46, 130.81, 129.37, 128.75, 128.51, 126.53, 42.18, 26.59, 20.24, 16.82. MS (ESI): 346.1 ($C_{15}H_{16}N_5O_3S$, $[M+H]^+$). Anal. Calcd for $C_{15}H_{15}N_5O_3S$: C, 52.16; H, 4.38; N, 20.28; Found: C, 52.24; H, 4.35; N, 20.31.

*4.1.1.3.*

*2-((2-(2-methyl-5-nitro-1H-imidazol-1-yl)ethyl)thio)-5-(p-tolyl)-1,3,4-oxadiazole (**11**)*

Light yellow crystals, yield: 61.1%, mp: 182-183 □. $^1$H NMR (300 MHz, $CDCl_3$) $\delta$: 2.44 (s, 3H), 2.60 (s, 3H), 3.65 (t, $J$ = 7.0 Hz, 2H), 4.83 (t, $J$ = 7.0 Hz, 2H), 7.32 (d, $J$ = 8.0 Hz, 2H), 7.90 (d, $J$ = 8.3 Hz, 2H), 7.98 (s, 1H). $^{13}$C NMR (100 MHz, $CDCl_3$) $\delta$: 162.34, 159.39, 149.72, 140.60, 139.65, 133.46, 129.10, 126.99, 125.47, 42.18, 26.59, 21.13, 16.82. MS (ESI): 346.1 ($C_{15}H_{16}N_5O_3S$, $[M+H]^+$). Anal. Calcd for $C_{15}H_{15}N_5O_3S$: C, 52.16; H, 4.38; N, 20.28; Found: C, 52.20; H, 4.34; N, 20.22.

*4.1.1.4.*

*2-(2-methoxyphenyl)-5-((2-(2-methyl-5-nitro-1H-imidazol-1-yl)ethyl)thio)-1,3,4-oxadiazole (**12**)*

Brown crystals, yield: 57.0%, mp: 155-156 □. $^1$H NMR (300 MHz, $CDCl_3$) $\delta$: 2.60 (s, 3H), 3.64 (t, $J$ = 7.1 Hz, 2H), 3.98 (s, 3H), 4.84 (t, $J$ = 7.1 Hz, 2H), 7.08 (t, $J$ = 7.4 Hz, 2H), 7.52 (dt, $J_1$ = 7.9 Hz, $J_2$ =1.6 Hz, 1H), 7.88 (dd, $J_1$ = 8.0 Hz, $J_2$ = 1.6 Hz, 1H), 7.97 (s, 1H). $^{13}$C NMR (100 MHz, $CDCl_3$) $\delta$: 162.34, 158.21, 151.42, 149.72, 139.65, 133.46, 131.99, 131.60, 120.56, 118.38, 115.31, 56.79, 42.18, 26.59, 16.82. MS (ESI): 362.1 ($C_{15}H_{16}N_5O_4S$, $[M+H]^+$). Anal. Calcd for $C_{15}H_{15}N_5O_4S$: C, 49.85; H, 4.18; N, 19.38; Found: C, 49.76; H, 4.17; N, 19.43.

*4.1.1.5.*

*2-(4-methoxyphenyl)-5-((2-(2-methyl-5-nitro-1H-imidazol-1-yl)ethyl)thio)-1,3,4-oxadiazole (**13**)*

Brown crystals, yield: 59.2%, mp: 171-172 □. $^1$H NMR (300 MHz, $CDCl_3$) $\delta$:

2.61 (s, 3H), 3.64 (t, $J$ = 7.0 Hz, 2H), 3.89 (s, 3H), 4.82 (t, $J$ = 7.0 Hz, 2H), 7.00-7.02 (d, $J$ = 9.0 Hz, 2H), 7.93-7.98 (m, 3H). $^{13}$C NMR (100 MHz, $CDCl_3$) $\delta$: 162.34, 162.19, 159.39, 149.72, 139.65, 133.46, 127.07, 121.55, 113.88, 56.04, 42.18, 26.59, 16.82. MS (ESI): 362.1 ($C_{15}H_{16}N_5O_4S$, $[M+H]^+$). Anal. Calcd for $C_{15}H_{15}N_5O_4S$: C, 49.85; H, 4.18; N, 19.38; Found: C, 49.83; H, 4.13; N, 19.42.

*4.1.1.6.*

*2-(5-((2-(2-methyl-5-nitro-1H-imidazol-1-yl)ethyl)thio)-1,3,4-oxadiazol-2-yl)aniline (**14**)*

Dark green crystals, yield: 72.9%, mp: 127-128 □. $^1$H NMR (500 MHz, $CDCl_3$) $\delta$: 2.62 (s, 3H), 3.68 (t, $J$ = 7.0 Hz, 2H), 4.85 (t, $J$ = 7.0 Hz, 2H), 5.85 (brs, 2H), 6.78-6.84 (m, 2H), 7.31 (t, $J$ = 7.8 Hz, 1H), 7.71 (d, $J$ = 8.0 Hz, 1H), 8.01 (s, 1H). $^{13}$C NMR (100 MHz, $CDCl_3$) $\delta$: 162.34, 150.82, 149.72, 144.39, 139.65, 133.46, 132.13, 125.59, 117.62, 117.43, 108.55, 42.18, 26.59, 16.82. MS (ESI): 347.1 ($C_{14}H_{15}N_6O_3S$, $[M+H]^+$). Anal. Calcd for $C_{14}H_{14}N_6O_3S$: C, 48.55; H, 4.07; N, 24.26; Found: C, 48.60; H, 4.01; N, 24.25.

*4.1.1.7.*

*4-(5-((2-(2-methyl-5-nitro-1H-imidazol-1-yl)ethyl)thio)-1,3,4-oxadiazol-2-yl)aniline (**15**)*

Brilliant yellow crystals, yield: 66.7%, mp: 212-213 □. $^1$H NMR (300 MHz, $CDCl_3$) $\delta$: 2.59 (s, 3H), 3.62 (t, $J$ = 7.0 Hz, 2H), 4.06 (brs, 2H), 4.81 (t, $J$ = 7.0 Hz, 2H), 6.73 (d, $J$ = 8.6 Hz, 2H), 7.79 (d, $J$ = 8.4 Hz, 2H), 7.97 (s, 1H). $^{13}$C NMR (100 MHz, $CDCl_3$) $\delta$: 162.34, 159.39, 156.25, 149.72, 139.65, 133.46, 127.68, 118.01, 114.55, 42.18, 26.59, 16.82. MS (ESI): 347.1 ($C_{14}H_{15}N_6O_3S$, $[M+H]^+$). Anal. Calcd for $C_{14}H_{14}N_6O_3S$: C, 48.55; H, 4.07; N, 24.26; Found: C, 48.61; H, 4.02; N, 24.29.

*4.1.1.8.*

*2-(2-ethoxyphenyl)-5-((2-(2-methyl-5-nitro-1H-imidazol-1-yl)ethyl)thio)-1,3,4-oxadiazole (**16**)*

Tan powder, yield: 66.2%, mp: 100-101 □. $^1$H NMR (500 MHz, $CDCl_3$) $\delta$: 1.50 (t, $J$ = 7.0 Hz, 3H), 2.61 (s, 3H), 3.67 (t, $J$ = 7.0 Hz, 2H), 4.22 (q , $J$ = 7.0 Hz, 2H), 4.86 (t, $J$ = 7.0 Hz, 2H), 7.06-7.10 (m, 2H), 7.52 (t, $J$ = 7.5 Hz, 1H), 7.91 (d, $J$ = 8.0 Hz, 1H), 8.00 (s, 1H). $^{13}$C NMR (100 MHz, $CDCl_3$) $\delta$: 162.34, 150.13, 149.72, 139.65, 134.72, 133.46, 129.88, 128.67, 128.66, 127.56, 73.21, 58.33, 42.18, 26.59, 16.82. MS (ESI): 376.1 ($C_{16}H_{18}N_5O_4S$, $[M+H]^+$). Anal. Calcd for $C_{16}H_{17}N_5O_4S$: C, 51.19; H, 4.56; N, 18.66; Found: C, 51.10; H, 4.53; N, 18.69.

*4.1.1.9.*

*2-(4-ethoxyphenyl)-5-((2-(2-methyl-5-nitro-1H-imidazol-1-yl)ethyl)thio)-1,3,4-oxadiazole (**17**)*

Light yellow crystals, yield: 67.2%, mp: 151-152 □. $^1$H NMR (500 MHz, $CDCl_3$) $\delta$: 1.48 (t, $J$ = 7.0 Hz, 3H), 2.63 (s, 3H), 3.66 (t, $J$ = 7.0 Hz, 2H), 4.14 (q, $J$ = 7.0 Hz, 2H), 4.85 (t, $J$ = 7.0 Hz, 2H), 7.02 (d, $J$ = 9.0 Hz, 2H), 7.95 (d, $J$ = 8.5 Hz, 2H), 8.01 (s, 1H). $^{13}$C NMR (100 MHz, $CDCl_3$) $\delta$: 162.34, 159.39, 149.72, 141.37, 139.65, 133.46, 130.94, 127.28, 126.95, 76.15, 58.33, 42.18, 26.59, 16.82. MS (ESI): 376.1 ($C_{16}H_{18}N_5O_4S$, $[M+H]^+$). Anal. Calcd for $C_{16}H_{17}N_5O_4S$: C, 51.19; H, 4.56; N, 18.66; Found: C, 51.26; H, 4.51; N, 18.71.

*4.1.1.10.*

*2-((2-(2-methyl-5-nitro-1H-imidazol-1-yl)ethyl)thio)-5-(2-nitrophenyl)-1,3,4-oxadiazole (**18**)*

Light yellow powder, yield: 48.5%, mp: 144-145 □. $^1$H NMR (500 MHz, $CDCl_3$) $\delta$: 2.62 (s, 3H), 3.69 (t, $J$ = 6.8 Hz, 2H), 4.85 (t, $J$ = 6.8 Hz, 2H), 7.80-7.84 (m, 2H), 7.95-7.96 (m, 1H), 8.02 (s, 1H), 8.11-8.13 (m, 1H). $^{13}$C NMR (100 MHz, $CDCl_3$) $\delta$: 162.34, 148.27, 146.01, 139.65, 133.93, 133.46, 132.32, 126.60, 126.12, 124.02, 42.18, 26.59, 16.82. MS (ESI): 377.1 ($C_{14}H_{13}N_6O_5S$, $[M+H]^+$). Anal. Calcd for $C_{14}H_{12}N_6O_5S$: C, 44.68; H, 3.21; N, 22.33; Found: C, 44.83; H, 3.15; N, 22.24.

*4.1.1.11.*

*2-((2-(2-methyl-5-nitro-1H-imidazol-1-yl)ethyl)thio)-5-(4-nitrophenyl)-1,3,4-oxadiazole (**19**)*

Yellow powder, yield: 63.5%, mp: 199-200 □. $^1$H NMR (500 MHz, $CDCl_3$) $\delta$: 2.62 (s, 3H), 3.72 (t, $J$ = 7.0 Hz, 2H), 4.86 (t, $J$ = 7.0 Hz, 2H), 8.01 (s, 1H), 8.24 (d, $J$ = 8.5 Hz, 2H), 8.42 (d, $J$ = 8.5 Hz, 2H). $^{13}$C NMR (100 MHz, $CDCl_3$) $\delta$: 162.34, 159.39, 147.39, 139.65, 133.46, 132.08, 127.45, 124.68, 42.18, 26.59, 16.82. MS (ESI): 377.1 ($C_{14}H_{13}N_6O_5S$, $[M+H]^+$). Anal. Calcd for $C_{14}H_{12}N_6O_5S$: C, 44.68; H, 3.21; N, 22.33; Found: C, 44.81; H, 3.20; N, 22.26.

*4.1.1.12.*

*2-(2-fluorophenyl)-5-((2-(2-methyl-5-nitro-1H-imidazol-1-yl)ethyl)thio)-1,3,4-oxadiazole (**20**)*

Grayish white powder, yield: 56.9%, mp: 110-111 □. $^1$H NMR (300 MHz, $CDCl_3$) $\delta$: 2.59 (s, 3H), 3.68 (t, $J$ = 7.1 Hz, 2H), 4.85 (t, $J$ = 7.1 Hz, 2H), 7.30-7.35 (m, 2H), 7.55-7.61 (m, 1H), 7.99-8.05 (m, 2H). $^{13}$C NMR (100 MHz, $CDCl_3$) $\delta$: 162.34, 161.60, 149.72, 149.13, 133.46, 127.48, 124.49, 117.68, 117.49, 42.18, 26.59, 16.82. MS (ESI): 350.1 ($C_{14}H_{13}FN_5O_3S$, $[M+H]^+$). Anal. Calcd for $C_{14}H_{12}FN_5O_3S$: C, 48.13; H, 3.46; N, 20.05; Found: C, 48.30; H, 3.51; N, 19.97.

*4.1.1.13.*

*2-(4-fluorophenyl)-5-((2-(2-methyl-5-nitro-1H-imidazol-1-yl)ethyl)thio)-1,3,4-oxadiazole (**21**)*

Light yellow crystals, yield: 43.5%, mp: 186-187 □. $^1$H NMR (500 MHz, $CDCl_3$) $\delta$: 2.63 (s, 3H), 3.68 (t, $J$ = 6.8 Hz, 2H), 4.84 (t, $J$ = 6.8 Hz, 2H), 7.24 (t, $J$ = 8.5 Hz, 2H), 8.00 (s, 1H), 8.03-8.06 (m, 2H). $^{13}$C NMR (100 MHz, $CDCl_3$) $\delta$: 165.21, 162.34, 159.39, 149.72, 133.46, 129.70, 123.55, 116.18, 42.18, 26.59, 16.82. MS (ESI): 350.1 ($C_{14}H_{13}FN_5O_3S$, $[M+H]^+$). Anal. Calcd for $C_{14}H_{12}FN_5O_3S$: C, 48.13; H, 3.46; N, 20.05; Found: C, 48.02; H, 3.46; N, 20.12.

*4.1.1.14.*

*2-(2-chlorophenyl)-5-((2-(2-methyl-5-nitro-1H-imidazol-1-yl)ethyl)thio)-1,3,4-oxadiazole (**22**)*

Reddish-brown powder, yield: 56.1%, mp: 107-108 □. $^1$H NMR (300 MHz, $CDCl_3$) $\delta$: 2.61 (s, 3H), 3.67 (t, $J$ = 7.0 Hz, 2H), 4.84 (t, $J$ = 7.0 Hz, 2H), 7.40-7.45 (m, 1H), 7.46-7.52 (m, 1H), 7.56-7.58 (m, 1H), 7.93-7.96 (m, 1H), 7.98 (s, 1H). $^{13}$C NMR (100 MHz, $CDCl_3$) $\delta$: 162.34, 149.72, 149.11, 139.65, 134.38, 133.46, 131.36, 131.12, 127.60, 127.11, 126.34, 42.18, 26.59, 16.82. MS (ESI): 366.0 ($C_{14}H_{13}ClN_5O_3S$, $[M+H]^+$). Anal. Calcd for $C_{14}H_{12}ClN_5O_3S$: C, 45.97; H, 3.31; N, 19.15; Found: C, 45.88; H, 3.32; N, 19.19.

*4.1.1.15.*

*2-(4-chlorophenyl)-5-((2-(2-methyl-5-nitro-1H-imidazol-1-yl)ethyl)thio)-1,3,4-oxadiazole (**23**)*

Light yellow powder, yield: 62.1%, mp: 205-207 □. $^1$H NMR (300 MHz, $CDCl_3$) $\delta$: 2.61 (s, 3H), 3.66 (t, $J$ = 7.1 Hz, 2H), 4.83 (t, $J$ = 7.1 Hz, 2H), 7.51 (d, $J$ = 6.9 Hz, 2H), 7.94-7.98 (m, 3H). $^{13}$C NMR (100 MHz, $CDCl_3$) $\delta$: 162.34, 159.39, 149.72, 139.65, 137.31, 133.46, 129.46, 128.39, 128.09, 42.18, 26.59, 16.82. MS (ESI): 366.0 ($C_{14}H_{13}ClN_5O_3S$, $[M+H]^+$). Anal. Calcd for $C_{14}H_{12}ClN_5O_3S$: C, 45.97; H, 3.31; N, 19.15; Found: C, 46.02; H, 3.28; N, 19.11.

*4.1.1.16.*

*2-(5-((2-(2-methyl-5-nitro-1H-imidazol-1-yl)ethyl)thio)-1,3,4-oxadiazol-2-yl)phenol (**24**)*

Light brown crystals, yield: 62.9%, mp: 159-160 □. $^1$H NMR (300 MHz, $CDCl_3$) $\delta$: 2.60 (s, 3H), 3.69 (t, $J$ = 6.9 Hz, 2H), 4.82 (t, $J$ = 6.9 Hz, 2H), 7.02 (t, $J$ = 7.9 Hz, 1H), 7.14 (d, $J$ = 7.9 Hz, 1H), 7.46 (t, $J$ = 7.9 Hz, 1H), 7.70 (dd, $J_1$ = 7.8 Hz, $J_2$ = 1.7 Hz, 1H), 7.98 (s, 1H), 9.74 (s, 1H). $^{13}$C NMR (100 MHz, $CDCl_3$) $\delta$: 162.34, 158.44, 149.72, 133.46, 130.12, 118.80, 111.70, 42.18, 26.59, 16.82. MS (ESI): 348.1 ($C_{14}H_{14}N_5O_4S$, $[M+H]^+$). Anal. Calcd for $C_{14}H_{13}N_5O_4S$: C, 48.41; H, 3.77; N, 20.16; Found: C, 48.32; H, 3.75; N, 20.12.

*4.1.1.17.*

*2-(4-isopropylphenyl)-5-((2-(2-methyl-5-nitro-1H-imidazol-1-yl)ethyl)thio)-1,3,4-oxadiazole (**25**)*

Light yellow crystals, yield: 67.8%, mp: 130-131 □. $^{1}$H NMR (500 MHz, $CDCl_3$) $\delta$: 1.31(d, $J$ = 7.0 Hz, 6H), 2.62 (s, 3H), 2.99-3.02 (m, 1H), 3.67 (t, $J$ = 6.8 Hz, 2H), 4.85 (t, $J$ = 6.8 Hz, 2H), 7.39 (d, $J$ = 8.0 Hz, 2H), 7.94-7.96 (m, 2H), 8.00 (s, 1H). $^{13}$C NMR (100 MHz, $CDCl_3$) $\delta$: 162.34, 159.39, 147.31, 139.65, 133.46, 129.60, 127.49, 125.42, 42.18, 34.20, 23.37, 16.82. MS (ESI): 374.1 ($C_{17}H_{20}N_5O_3S$, $[M+H]^+$). Anal. Calcd for $C_{17}H_{19}N_5O_3S$: C, 54.68; H, 5.13; N, 18.75; Found: C, 54.70; H, 5.12; N, 18.78.

*4.1.1.18.*

*2-(4-(tert-butyl)phenyl)-5-((2-(2-methyl-5-nitro-1H-imidazol-1-yl)ethyl)thio)-1,3,4-oxadiazole (**26**)*

Light yellow crystals, yield: 58.7%, mp: 167-168 □. $^{1}$H NMR (300 MHz, $CDCl_3$) $\delta$: 1.36 (s, 9H), 2.60 (s, 3H), 3.65 (t, $J$ = 7.1 Hz, 2H), 4.83 (t, $J$ = 7.1 Hz, 2H), 7.53 (d, $J$ = 8.4 Hz, 2H), 7.92-7.98 (m, 3H). $^{13}$C NMR (100 MHz, $CDCl_3$) $\delta$: 162.34, 159.39, 153.17, 149.72, 139.65, 133.46, 128.94, 126.90, 126.42, 42.18, 31.44, 26.59, 16.82. MS (ESI): 388.1 ($C_{18}H_{22}N_5O_3S$, $[M+H]^+$). Anal. Calcd for $C_{18}H_{21}N_5O_3S$: C, 55.80; H, 5.46; N, 18.08; Found: C, 55.71; H, 5.48; N, 18.11.

*4.1.1.19.*

*N,N-dimethyl-4-(5-((2-(2-methyl-5-nitro-1H-imidazol-1-yl)ethyl)thio)-1,3,4-oxadiazol-2-yl)aniline (**27**)*

Brilliant yellow crystals, yield: 53.6%, mp: 184-185 □. $^{1}$H NMR (300 MHz, $CDCl_3$) $\delta$: 2.60 (s, 3H), 3.06 (s, 6H), 3.62 (t, $J$ = 6.9 Hz, 2H), 4.82 (t, $J$ = 6.9 Hz, 2H), 6.73 (d, $J$ = 8.6 Hz, 2H), 7.84 (d, $J$ = 8.8 Hz, 2H), 7.98 (s, 1H). $^{13}$C NMR (100 MHz, $CDCl_3$) $\delta$: 162.34, 159.39, 157.16, 149.72, 133.46, 127.55, 118.60, 111.14, 42.18, 41.91, 26.59, 16.82. MS (ESI): 375.1 ($C_{16}H_{19}N_6O_3S$, $[M+H]^+$). Anal. Calcd for

$C_{16}H_{18}N_6O_3S$: C, 51.33; H, 4.85; N, 22.45; Found: C, 51.25; H, 4.86; N, 22.41.

*4.1.1.20.*

*2-methyl-6-(5-((2-(2-methyl-5-nitro-1H-imidazol-1-yl)ethyl)thio)-1,3,4-oxadiazol-2-yl)phenol (**28**)*

Brown crystals, yield: 60.0%, mp: 163-164 □. $^1$H NMR (500 MHz, $CDCl_3$) $\delta$: 2.37 (s, 3H), 2.62 (s, 3H), 3.71 (t, $J$ = 7.0 Hz, 2H), 4.85 (t, $J$ = 7.0 Hz, 2H), 6.94 (t, $J$ = 7.5 Hz, 1H), 7.35 (d, $J$ = 7.0 Hz, 1H), 7.58 (d, $J$ = 7.5 Hz, 1H), 8.01 (s, 1H), 9.92 (s, 1H). $^{13}$C NMR (100 MHz, $CDCl_3$) $\delta$: 162.34, 155.83, 149.72, 139.65, 126.96, 118.86, 111.54, 42.18, 26.59, 15.70, 16.82. MS (ESI): 362.1 ($C_{15}H_{16}N_5O_4S$, $[M+H]^+$). Anal. Calcd for $C_{15}H_{15}N_5O_4S$: C, 49.85; H, 4.18; N, 19.38; Found: C, 50.02; H, 4.25; N, 19.31.

*4.1.1.21.*

*5-methyl-2-(5-((2-(2-methyl-5-nitro-1H-imidazol-1-yl)ethyl)thio)-1,3,4-oxadiazol-2-yl)phenol (**29**)*

Brown crystals, yield: 66.1%, mp: 176-178 □. $^1$H NMR (500 MHz, $CDCl_3$) $\delta$: 2.41 (s, 3H), 2.62 (s, 3H), 3.70 (t, $J$ = 7.0 Hz, 2H), 4.85 (t, $J$ = 7.0 Hz, 2H), 6.86 (d, $J$ = 8.0 Hz, 1H), 6.97 (s, 1H), 7.60 (d, $J$ = 8.5 Hz, 1H), 8.01 (s, 1H), 9.69 (s, 1H). $^{13}$C NMR (100 MHz, $CDCl_3$) $\delta$: 162.34, 157.81, 149.72, 139.65, 129.27, 120.30, 112.36, 42.18, 26.59, 21.21, 16.82. MS (ESI): 362.1 ($C_{15}H_{15}N_5O_4S$, $[M+H]^+$). Anal. Calcd for $C_{15}H_{15}N_5O_4S$: C, 49.85; H, 4.18; N, 19.38; Found: C, 49.96; H, 4.21; N, 19.29.

*4.1.1.22.*

*5-methoxy-2-(5-((2-(2-methyl-5-nitro-1H-imidazol-1-yl)ethyl)thio)-1,3,4-oxadiazol-2-yl)phenol (**30**)*

Brown powder, yield: 40.8%, mp: 180-181 □. $^1$H NMR (500 MHz, $CDCl_3$) $\delta$: 2.63 (s, 3H), 3.69 (t, $J$ = 6.5 Hz, 2H), 3.88 (s, 3H), 4.84 (t, $J$ = 6.5 Hz, 2H), 6.61 (d, $J$ = 8.5 Hz, 1H), 6.65 (s, 1H), 7.62 (d, $J$ = 9.0 Hz, 1H), 8.02 (s, 1H), 9.88 (s, 1H). $^{13}$C NMR (100 MHz, $CDCl_3$) $\delta$: 162.34, 160.53, 159.84, 149.72, 139.65, 133.46, 130.30,

109.80, 106.85, 103.04, 56.04, 42.18, 26.59, 16.82. MS (ESI): 378.1 ($C_{15}H_{16}N_5O_5S$, $[M+H]^+$). Anal. Calcd for $C_{15}H_{15}N_5O_5S$: C, 47.74; H, 4.01; N, 18.56; Found: C, 47.89; H, 4.08; N, 18.48.

*4.1.1.23.*

*2-(3,5-dimethoxyphenyl)-5-((2-(2-methyl-5-nitro-1H-imidazol-1-yl)ethyl)thio)-1,3,4-oxadiazole (**31**)*

Milky-white crystals, yield: 47.0%, mp: 164-166 □. $^1$H NMR (500 MHz, $CDCl_3$) $\delta$: 2.63 (s, 3H), 3.68 (t, $J$ = 6.5 Hz, 2H), 3.87 (s, 6H), 4.85 (t, $J$ = 6.3 Hz, 2H), 6.66 (s, 1H), 7.17 (s, 2H), 8.01 (s, 1H). $^{13}$C NMR (100 MHz, $CDCl_3$) $\delta$: 163.18, 162.34, 159.35, 149.72, 133.46, 125.65, 107.95, 106.36, 56.04, 42.18, 26.59, 16.82. MS (ESI): 392.1 ($C_{16}H_{18}N_5O_5S$, $[M+H]^+$). Anal. Calcd for $C_{16}H_{17}N_5O_5S$: C, 49.10; H, 4.38; N, 17.89; Found: C, 48.91; H, 4.30; N, 17.83.

*4.1.1.24.*

*2-((2-(2-methyl-5-nitro-1H-imidazol-1-yl)ethyl)thio)-5-(3,4,5-trimethoxyphenyl)-1,3,4-oxadiazole (**32**)*

Light yellow powder, yield: 51.2%, mp: 154-155 □. $^1$H NMR (500 MHz, $CDCl_3$) $\delta$: 2.64 (s, 3H), 3.68 (t, $J$ = 7.3 Hz, 2H), 3.95 (s, 9H), 4.86 (t, $J$ = 7.3 Hz, 2H), 7.26 (s, 2H), 8.01 (s, 1H). $^{13}$C NMR (100 MHz, $CDCl_3$) $\delta$: 162.34, 159.35, 151.61, 139.65, 133.46, 122.02, 107.03, 60.65, 56.79, 42.18, 26.59, 16.82. MS (ESI): 422.1 ($C_{17}H_{20}N_5O_6S$, $[M+H]^+$). Anal. Calcd for $C_{17}H_{19}N_5O_6S$: C, 48.45; H, 4.54; N, 16.62; Found: C, 48.36; H, 4.50; N, 16.71.

*4.1.1.25.*

*2-(furan-2-yl)-5-((2-(2-methyl-5-nitro-1H-imidazol-1-yl)ethyl)thio)-1,3,4-oxadiazole (**33**)*

Brown crystals, yield: 68.7%, mp: 119-120 □. $^1$H NMR (300 MHz, $CDCl_3$) $\delta$: 2.59 (s, 3H), 3.65 (t, $J$ = 7.0 Hz, 2H), 4.82 (t, $J$ = 7.0 Hz, 2H), 6.60-6.62 (m, 1H), 7.16 (d, $J$ = 3.5 Hz, 1H), 7.65-7.66 (m, 1H), 7.98 (s, 1H). $^{13}$C NMR (100 MHz, $CDCl_3$)

$\delta$: 163.79, 150.65, 149.93, 149.72, 144.04, 139.65, 133.46, 112.60, 111.21, 42.18, 26.59, 16.82. MS (ESI): 322.1 ($C_{12}H_{12}N_5O_4S$, $[M+H]^+$). Anal. Calcd for $C_{12}H_{11}N_5O_4S$: C, 44.86; H, 3.45; N, 21.80; Found: C, 44.79; H, 3.45; N, 21.77.

*4.1.1.26.*

*2-((2-(2-methyl-5-nitro-1H-imidazol-1-yl)ethyl)thio)-5-(thiophen-2-yl)-1,3,4-oxadiazole (**34**)*

Brown crystals, yield: 63.4%, mp: 123-124 □. $^1$H NMR (300 MHz, $CDCl_3$) $\delta$: 2.60 (s, 3H), 3.64 (t, $J$ = 7.1 Hz, 2H), 4.81 (t, $J$ = 7.1 Hz, 2H), 7.17-7.20 (m, 1H), 7.57-7.59 (m, 1H), 7.72-7.74 (m, 1H), 7.98 (s, 1H). $^{13}$C NMR (100 MHz, $CDCl_3$) $\delta$: 163.79, 163.78, 149.72, 139.65, 133.46, 131.30, 130.54, 130.05, 127.41, 42.18, 26.59, 16.82. MS (ESI): 338.0 ($C_{12}H_{12}N_5O_3S_2$, $[M+H]^+$). Anal. Calcd for $C_{12}H_{11}N_5O_3S_2$: C, 42.72; H, 3.29; N, 20.76; Found: C, 42.75; H, 3.30; N, 20.80.

*4.1.1.27.*

*2-((2-(2-methyl-5-nitro-1H-imidazol-1-yl)ethyl)thio)-5-(pyridin-2-yl)-1,3,4-oxadiazole (**35**)*

Brown crystals, yield: 46.2%, mp: 154-155 □. $^1$H NMR (300 MHz, $CDCl_3$) $\delta$: 2.61 (s, 3H), 3.69 (t, $J$ = 7.0 Hz, 2H), 4.83 (t, $J$ = 7.0 Hz, 2H), 7.46-7.50 (m, 1H), 7.90 (dt, $J_1$ = 7.9 Hz, $J_2$ =1.8 Hz, 1H), 7.97 (s, 1H), 8.20 (d, $J$ = 8.0 Hz, 1H), 8.78 (d, $J$ = 4.2 Hz, 1H). $^{13}$C NMR (100 MHz, $CDCl_3$) $\delta$: 162.34, 161.29, 149.72, 148.47, 142.58, 139.65, 133.46, 128.49, 119.84, 42.18, 26.59, 16.82. MS (ESI): 333.1 ($C_{13}H_{13}N_6O_3S$, $[M+H]^+$). Anal. Calcd for $C_{13}H_{12}N_6O_3S$: C, 46.98; H, 3.64; N, 25.29; Found: C, 47.12; H, 3.56; N, 25.22.

*4.1.1.28.*

*2-((2-(2-methyl-5-nitro-1H-imidazol-1-yl)ethyl)thio)-5-(pyridin-3-yl)-1,3,4-oxadiazole (**36**)*

Reddish-brown crystals, yield: 57.1%, mp: 156-158 □. $^1$H NMR (300 MHz, $CDCl_3$) $\delta$: 2.61 (s, 3H), 3.68 (t, $J$ = 7.0 Hz, 2H), 4.84 (t, $J$ = 7.0 Hz, 2H), 7.46-7.50

(m, 1H), 7.98 (s, 1H), 8.28-8.32 (m, 1H), 8.81 (s, 1H), 9.25 (s, 1H). $^{13}$C NMR (100 MHz, $CDCl_3$) $\delta$: 162.34, 149.72, 148.34, 139.65, 135.74, 133.46, 128.39, 123.63, 42.18, 26.59, 16.82. MS (ESI): 333.1 ($C_{13}H_{13}N_6O_3S$, $[M+H]^+$). Anal. Calcd for $C_{13}H_{12}N_6O_3S$: C, 46.98; H, 3.64; N, 25.29; Found: C, 46.92; H, 3.60; N, 25.32.

*4.1.1.29.*

*3-(5-((2-(2-methyl-5-nitro-1H-imidazol-1-yl)ethyl)thio)-1,3,4-oxadiazol-2-yl)pyridin -4-amine (**37**)*

Light yellow crystals, yield: 45.9%, mp: 216-218 □. $^1$H NMR (500 MHz, $CDCl_3$) $\delta$: 2.63 (s, 3H), 3.71 (t, $J$ = 7.0 Hz, 2H), 4.85 (t, $J$ = 6.8 Hz, 2H), 6.28 (brs, 2H), 6.70 (d, $J$ = 6.5 Hz, 1H), 8.01 (s, 1H), 8.28 (d, $J$ = 6.0 Hz, 1H), 8.82 (s, 1H). $^{13}$C NMR (100 MHz, $CDCl_3$) $\delta$: 163.37, 162.34, 151.35, 148.77, 142.51, 139.65, 133.46, 110.32, 108.89, 42.18, 26.59, 16.82. MS (ESI): 348.1 ($C_{13}H_{14}N_7O_3S$, $[M+H]^+$). Anal. Calcd for $C_{13}H_{13}N_7O_3S$: C, 44.95; H, 3.77; N, 28.23; Found: C, 45.09; H, 3.69; N, 28.22.

*4.1.1.30.*

*5-(5-((2-(2-methyl-5-nitro-1H-imidazol-1-yl)ethyl)thio)-1,3,4-oxadiazol-2-yl)pyridin -2-amine (**38**)*

Brilliant yellow powder, yield: 48.5%, mp: 153-154 □. $^1$H NMR (500 MHz, $CDCl_3$) $\delta$: 2.63 (s, 3H), 3.67 (t, $J$ = 7.0 Hz, 2H), 4.85 (t, $J$ = 7.3 Hz, 2H), 4.94 (s, 2H), 6.61 (d, $J$ = 8.5 Hz, 1H), 8.01 (s, 1H), 8.05 (d, $J$ = 8.5 Hz, 1H), 8.72 (s, 1H). $^{13}$C NMR (100 MHz, $CDCl_3$) $\delta$: 162.34, 161.95, 154.91, 149.72, 147.64, 139.65, 136.12, 133.46, 117.19, 106.54, 42.18, 26.59, 16.82. MS (ESI): 348.1 ($C_{13}H_{14}N_7O_3S$, $[M+H]^+$). Anal. Calcd for $C_{13}H_{13}N_7O_3S$: C, 44.95; H, 3.77; N, 28.23; Found: C, 44.81; H, 3.81; N, 28.33.

*4.1.1.31.*

*2-((2-(2-methyl-5-nitro-1H-imidazol-1-yl)ethyl)thio)-5-(pyridin-4-yl)-1,3,4-oxadiazole (**39**)*

Light yellow crystals, yield: 56.9%, mp: 172-173 □. $^1$H NMR (300 MHz, $CDCl_3$)

$\delta$: 2.61 (s, 3H), 3.70 (t, $J$ = 7.0 Hz, 2H), 4.83 (t, $J$ = 7.0 Hz, 2H), 7.86-7.88 (d, $J$ = 5.7 Hz, 2H), 7.98 (s, 1H), 8.84 (s, 2H). $^{13}$C NMR (100 MHz, $CDCl_3$) $\delta$: 162.34, 159.39, 150.31, 149.72, 139.65, 133.37, 133.46, 123.42, 42.18, 26.59, 16.82. MS (ESI): 333.1 ($C_{13}H_{13}N_6O_3S$, $[M+H]^+$). Anal. Calcd for $C_{13}H_{12}N_6O_3S$: C, 46.98; H, 3.64; N, 25.29; Found: C, 47.01; H, 3.62; N, 25.27.

*4.1.1.32.*

*4-(5-((2-(2-methyl-5-nitro-1H-imidazol-1-yl)ethyl)thio)-1,3,4-oxadiazol-2-yl)pyridin-2-amine (**40**)*

Light yellow powder, yield: 41.9%, mp: 217-218 □. $^1$H NMR (500 MHz, $CDCl_3$) $\delta$: 2.63 (s, 3H), 3.70 (t, $J$ = 7.0 Hz, 2H), 4.84 (t, $J$ = 6.8 Hz, 2H), 4.88 (s, 2H), 7.11 (s, 1H), 7.23 (d, $J$ = 5.0 Hz, 1H), 8.00 (s, 1H), 8.25 (d, $J$ = 5.5 Hz, 1H). $^{13}$C NMR (100 MHz, $CDCl_3$) $\delta$: 162.34, 160.38, 159.57, 150.20, 149.72, 139.65, 134.07, 133.46, 112.98, 109.02, 42.18, 26.59, 16.82. MS (ESI): 348.1 ($C_{13}H_{14}N_7O_3S$, $[M+H]^+$). Anal. Calcd for $C_{13}H_{13}N_7O_3S$: C, 44.95; H, 3.77; N, 28.23; Found: C, 44.82; H, 3.80; N, 28.31.

*4.1.1.33.*

*2-(2-chloropyridin-4-yl)-5-((2-(2-methyl-5-nitro-1H-imidazol-1-yl)ethyl)thio)-1,3,4-oxadiazole (**41**)*

Light yellow powder, yield: 57.5%, mp: 161-163 □. $^1$H NMR (500 MHz, $CDCl_3$) $\delta$: 2.63 (s, 3H), 3.73 (t, $J$ = 7.0 Hz, 2H), 4.85 (t, $J$ = 7.0 Hz, 2H), 7.83 (d, $J$ = 5.5 Hz, 1H), 7.94 (s, 1H), 8.01 (s, 1H), 8.63 (d, $J$ = 5.5 Hz, 1H). $^{13}$C NMR (100 MHz, $CDCl_3$) $\delta$: 162.34, 159.57, 152.36, 151.13, 149.72, 139.65, 135.93, 133.46, 124.81, 123.09, 42.18, 26.59, 16.82. MS (ESI): 367.0 ($C_{13}H_{12}ClN_6O_3S$, $[M+H]^+$). Anal. Calcd for $C_{13}H_{11}ClN_6O_3S$: C, 42.57; H, 3.02; N, 22.91; Found: C, 42.70; H, 2.95; N, 22.83.

*4.1.1.34.*

*2-((2-(2-methyl-5-nitro-1H-imidazol-1-yl)ethyl)thio)-5-(naphthalen-1-yl)-1,3,4-oxadiazole (**42**)*

Brown crystals, yield: 72.9%, mp: 155-157 □. $^1$H NMR (500 MHz, $CDCl_3$) $\delta$: 2.67 (s, 3H), 3.74 (t, $J$ = 7.3 Hz, 2H), 4.91 (t, $J$ = 7.0 Hz, 2H), 7.60-7.66 (m, 2H), 7.72-7.75 (m, 1H), 7.98 (d, $J$ = 8.5 Hz, 1H), 8.02 (s, 1H), 8.08 (d, $J$ = 8.0 Hz, 1H), 8.17 (d, $J$ = 8.0 Hz, 1H), 9.20 (d, $J$ = 8.5 Hz, 1H). $^{13}$C NMR (100 MHz, $CDCl_3$) $\delta$: 162.34, 152.33, 149.72, 139.65, 135.93, 133.28, 133.46, 131.10, 128.28, 128.24, 127.95, 127.34, 125.88, 125.81, 125.01, 124.39, 42.18, 26.59, 16.82. MS (ESI): 382.1 ($C_{18}H_{16}N_5O_3S$, $[M+H]^+$). Anal. Calcd for $C_{18}H_{15}N_5O_3S$: C, 56.68; H, 3.96; N, 18.36; Found: C, 56.71; H, 3.98; N, 18.39.

*4.1.1.35.*

*2-((2-(2-methyl-5-nitro-1H-imidazol-1-yl)ethyl)thio)-5-(naphthalen-2-yl)-1,3,4-oxadiazole (**43**)*

Light brown powder, yield: 41.8%, mp: 167-168 □. $^1$H NMR (500 MHz, $CDCl_3$) $\delta$: 2.66 (s, 3H), 3.71 (t, $J$ = 7.0 Hz, 2H), 4.88 (t, $J$ = 7.0 Hz, 2H), 7.61-7.64 (m, 2H), 7.93 (d, $J$ = 7.5 Hz, 1H), 7.98-8.02 (m, 3H), 8.12 (d, $J$ = 8.5 Hz, 1H). $^{13}$C NMR (100 MHz, $CDCl_3$) $\delta$: 162.34, 160.11, 149.72, 139.65, 134.51, 134.02, 133.46, 130.64, 129.70, 129.33, 128.22, 127.00, 126.52, 125.93, 122.41, 42.18, 26.59, 16.82. MS (ESI): 382.1 ($C_{18}H_{16}N_5O_3S$, $[M+H]^+$). Anal. Calcd for $C_{18}H_{15}N_5O_3S$: C, 56.68; H, 3.96; N, 18.36; Found: C, 56.81; H, 4.00; N, 18.31.

*4.1.1.36.*

*2-(2,3-dihydrobenzo[b][1,4]dioxin-6-yl)-5-((2-(2-methyl-5-nitro-1H-imidazol-1-yl)ethyl)thio)-1,3,4-oxadiazole (**44**)*

Grayish white crystals, yield: 60.5%, mp: 173-174 □. $^1$H NMR (500 MHz, $CDCl_3$) $\delta$: 2.62 (s, 3H), 3.66 (t, $J$ = 7.3 Hz, 2H), 4.33-4.36 (m, 4H), 4.84 (t, $J$ = 7.0 Hz, 2H), 7.00 (d, $J$ = 8.5 Hz, 1H), 7.52-7.54 (m, 2H), 8.01 (s, 1H). $^{13}$C NMR (100 MHz, $CDCl_3$) $\delta$: 162.34, 159.57, 149.94, 149.72, 145.95, 139.65, 133.46, 120.41, 119.59, 117.45, 113.31, 61.31, 42.18, 26.59, 16.82. MS (ESI): 390.1 ($C_{16}H_{16}N_5O_5S$, $[M+H]^+$). Anal. Calcd for $C_{16}H_{15}N_5O_5S$: C, 49.35; H, 3.88; N, 17.99; Found: C, 49.51; H, 3.91; N, 18.02.

*4.1.2. Crystallographic Studies*

X-ray single-crystal diffraction data of compound **9** were collected on a Bruker SMARTAPEX CCD diffractometer at 293(2) K using Mo Kα radiation (λ = 0.71073 Å) by the ω scan mode. The program SAINT was used for the integration of the diffraction profiles. All the structures were solved by direct methods using the SHELXS program of the SHELXTL package and refined by full-matrix least-squares methods with SHELXL-97.[31] All non-hydrogen atoms of compound **9** were refined with anisotropic thermal parameters. All hydrogen atoms were placed in geometrically idealized positions and constrained to ride on their parent atoms.

*4.2. Anti-proliferation assay*

The *in vitro* anticancer activities of the prepared compounds **9-44** against HepG2, SGC-7901, and MCF-7 cell lines were evaluated as described in the literature[32] with some modifications. Target tumor cells grew to log phase in *RPMI 1640* medium supplemented with 10% fetal bovine serum. After reaching a dilution of $3\times10^4$ cells $mL^{-1}$ with the medium, 100 $\mu$L of the obtained cell suspension was added to each well of 96-well culture plates. Subsequently, incubation was performed at 37 ˚C in 5% $CO_2$ atmosphere for 24 h before the cytotoxicity assessment. Testing samples at pre-set concentrations were added to 6 wells with 5-FU being employed as a positive reference. After 48 h exposure period, 25 $\mu$L of PBS containing 2.5 mg $mL^{-1}$ of MTT was added to each well. After 4 h, the medium was replaced by 150 $\mu$L DMSO to dissolve the purple formazan crystals produced. The absorbance at 570 nm of each well was measured on an ELISA plate reader. The data represented the mean of three independent experiments in triplicate and were expressed as means ± SD. The $IC_{50}$ value was defined as the concentration at which 50% of the cells could survive.

*4.3. Thymidylate Synthase Assay*

TS was assayed spectrophotometrically at 30° and pH 7.4 in a mixture containing 0.1 M 2-mercaptoethanol, 0.0003 M (6R,S)-tetrahydrofolate, 0.012 M

formaldehyde, 0.02 M $MgCl_2$, 0.001 M dUMP, 0.04 M TrisHCl, and 0.00075 M NaEDTA.

This was the assay described by A. J. Wahba and M.Friedkin,[33a] except that the dUMP concentration was increased 25-fold as per V. J. Davisson, W. Sirawaraporn, and D. V. Santi.[33b] The reaction was initiated by the addition of an amount of enzyme yielding a change in absorbance at 340 nm of 0.016/min in the absence of inhibitor. The percent inhibition was determined at a minimum of four inhibitor concentrations within 20% of the 50% point. The standard deviations for determination of the 50% points were within ±10% of the values given.

*4.4. Bacterial suppressive assay*

The antibacterial activity of compounds **18**, **37**, and **40** was tested against *E. coli* ATCC 25922, *Pseudomonas aeruginosa* ATCC 27853, *Staphylococcus aureus* ATCC 6538 and *Bacillus subtilis* ATCC 530 using MH medium (Mueller-Hinton medium: casein hydrolysate 17.5 g, soluble starch 1.5 g, beef extract 1000 mL). The MIC values of the tested compounds were determined by a colorimetric method using the dye MTT (3-(4, 5-Dimethylthiazol-2-yl)-2, 5-diphenyltetrazolium bromide). A stock solution of the synthesized compound (100 $\mu$g/mL) in DMSO was prepared, and graded quantities of the tested compounds were incorporated in specified quantity of sterilized liquid MH medium. A specified quantity of the medium containing the compound was poured into microtitration plates. Suspension of the microorganism was prepared to approximately $10^5$ cfu/mL and applied to microtitration plates with serially diluted compounds in DMSO, and then they were incubated at 37 ℃ for 24 h. After the MICs were visually determined on each of the microtitration plates, 50 $\mu$L of PBS (phosphate buffered saline 0.01 mol/L, pH 7.4: $Na_2HPO_4$•$12H_2O$ 2.9 g, $KH_2PO_4$ 0.2 g, NaCl 8.0 g, KCl 0.2 g, distilled water 1000 mL) containing 2 mg of MTT/mL was added to each well. Incubation was continued at room temperature for 4–5 h. The content of each well was removed, and 100 $\mu$L of isopropanol containing 5% 1 mol/L HCl was added to extract the dye. After 12 h of incubation at room

temperature, the optical density (OD) was measured with a microplate reader at 550 nm.

*4.5. Experimental protocol of docking study*

Molecular docking of compound **18** into the three dimensional X-ray structure of human TS and *E. coli* TS (PDB code: 1HVY and 2KCE, respectively) was carried out using the Discovery Studio (version 3.1) as implement through the graphical user interface DS- CDOCKER protocol.

The three-dimensional structures of the aforementioned compounds were constructed using Chem. 3D ultra 12.0 software [Chemical Structure Drawing Standard; Cambridge Soft corporation, USA (2010)], then they were energetically minimized by using MMFF94 with 5000 iterations and minimum RMS gradient of 0.10. The crystal structures of two TS proteins complexes were retrieved from the RCSB Protein Data Bank (http://www.rcsb.org/pdb/home/home.do). All bound waters and ligands were eliminated from the protein and the polar hydrogen was added to the proteins.

*4.6. 3D-QSAR*

Ligand-based 3D-QSAR approach was performed by QSAR software of DS 3.1 (Discovery Studio 3.1, Accelrys, Co. Ltd). The training sets were composed of 29 inhibitors with the corresponding $pIC_{50}$ values which were converted from the obtained $IC_{50}$ ($\mu$M), and test sets comprised 7 compounds of data sets as list in **Table 5**. All the definition of the descriptors can be seen in the Help of DS 3.1 software and they were calculated by QSAR protocol of DS 3.1.[34] The alignment conformation of each molecule was the one with lowest interaction energy in the docked results of CDOCKER (generated in part *4.5*). The predictive ability of 3D-QSAR modeling could be evaluated based on the cross-validated correlation coefficient, which qualified the predictive ability of the models. Scrambled test (Y scrambling) was performed to investigate the risk of chance correlations. The inhibitory potencies of compounds were randomly reordered for 30 times and subject to leave-one-out validation test, respectively. The models were also validated by test sets, in which the

compounds are not included in the training sets. Usually, one can believe that the modeling is reliable, when the $r^2$ for test sets is larger than 0.6, respectively.

**Acknowledgements**

This work was supported by Jiangsu National Science Foundation (No. BK2009239) and the Fundamental Research Fund for the Central Universities (No. 1092020804).

**References and Notes**

1. Garg, D.; Henrich, S.; Salo-Ahen, O. M.; Myllykallio, H.; Costi, M. P.; Wade, R. C. *J. Med. Chem.* **2010**, *53*, 6539.
2. Hardy, L. W.; Finer-Moore, J. S.; Montfort, W. R.; Jones, M. O.; Santi, D. V.; Stroud, R. M. *Science* **1987**, *235*, 448.
3. Berman, E. M.; Werbel, L. M. *J. Med. Chem.* **1991**, *34*, 479.
4. Gangjee, A.; Elzein, E.; Kothare, M.; Vasudevan, A. *Curr. Pharm. Design* **1996**, *2*, 263.
5. Chattopadhyay, S.; Moran, R. G.; Goldman, I. D. *Mol. Cancer Ther.* **2007**, *6*, 404.
6. Peters, G. J.; van Triest, B.; Backus, H.; Kuiper, C. M.; van der Wilt, C. L.; Pinedo, H. M. *Eur. J. Cancer* **2000**, *36*, 916.
7. Taylor, E. C.; Kuhnt, D.; Shih, C.; Rinzel, S. M.; Grindey, G. B.; Barredo, J.; Jannatipour, M.; Moran, R. G. *J. Med. Chem*. **1992**, *35*, 4450.
8. Gangjee, A.; Jain, H. D.; Kisliuk, R. L. *Bioorg. Med. Chem. Lett.* **2005**, *15*, 2225.
9. Creaven, P. J.; Pendyala, L.; Meropol, N. J.; Clendeninn, N. J.; Wu, E. Y.; Loewen, G. M.; Proefrock, A.; Johnston, A.; Dixon, M. *Cancer Chemother Pharmacol* **1998**, *41*, 167.
10. Gangjee, A.; Zaware, N.; Raghavan, S.; Ihnat, M.; Shenoy, S.; Kisliuk, R. L. *J. Med. Chem*. **2010**, *53,* 1563.
11. Gangjee, A.; Li, W.; Kisliuk, R. L.; Cody, V.; Pace, J.; Piraino, J.; Makin, J. *J.*

*Med. Chem.* **2009**, *52*, 4892.

12. Saitoh, M.; Kunitomo, J.; Kimura, E.; Iwashita, H.; Uno, Y.; Onishi, T.; Uchiyama, N.; Kawamoto, T.; Tanaka, T.; Mol, C. D.; Dougan, D. R.; Textor, G. P.; Snell, G. P.; Takizawa, M.; Itoh, F.; Kori, M. *J. Med. Chem.* **2009**, *52*, 6270.
13. Lee, S. H.; Seo, H. J.; Lee, S. H.; Jung, M. E.; Park, J. H.; Park, H. J.; Yoo, J.; Yun, H.; Na, J.; Kang, S. Y.; Song, K. S.; Kim, M. A.; Chang, C. H.; Kim, J.; Lee, J. *J. Med. Chem.* **2008**, *51*, 7216.
14. Rai, N. P.; Narayanaswamy, V. K.; Shashikanth, S.; Arunachalam, P. N. *Eur. J. Med. Chem.* **2009**, *44*, 4522.
15. Kadi, A. A.; El-Brollosy, N. R.; Al-Deeb, O. A.; Habib, E. E.; Ibrahim, T. M.; El-Emam, A. A. *Eur. J. Med. Chem.* **2007**, *42*, 235.
16. Pinna, G. A.; Murineddu, G.; Murruzzu, C.; Zuco, V.; Zunino, F.; Cappelletti, G.; Artali, R.; Cignarella, G.; Solano, L.; Villa, S. *ChemMedChem* **2009**, *4*, 998.
17. Abadi, A. H.; Eissa, A. A.; Hassan, G. S. *Chem Pharm Bull (Tokyo)* **2003**, *51*, 838.
18. Guimaraes, C. R.; Boger, D. L.; Jorgensen, W. L. *J. Am. Chem. Soc.* **2005**, *127*, 17377.
19. (a) Lau, A. H.; Lam, N. P.; Piscitelli, S. C.; Wilkes, L.; Danziger, L. H. *Clin. Pharmacokinet.* **1992**, *23*, 328; (b) Uto, Y.; Nagasawa, H.; Jin, C. Z.; Nakayama, S.; Tanaka, A.; Kiyoi, S.; Nakashima, H.; Shimamura, M.; Inayama, S.; Fujiwara, T.; Takeuchi, Y.; Uehara, Y.; Kirk, K. L.; Nakata, E.; Hori, H. *Bioorg. Med. Chem.* **2008**, *16*, 6042.
20. Mallia, M. B.; Mathur, A.; Subramanian, S.; Banerjee, S.; Sarma, H. D.; Venkatesh, M. *Bioorg. Med. Chem. Lett.* **2005**, *15*, 3398.
21. Born, J. L.; Smith, B. R.; Harper, N.; Koch, C. J. *Biochem. Pharmacol.* **1992**, *43*, 1337.
22. Lord, E. M.; Harwell, L.; Koch, C. J. *Cancer Res.* **1993**, *53*, 5721.
23. Webster, L. T. Drugs Used in the Chemotherapy of Protozoal Infections. In The Pharmacological Basis of Therapeutics, 8th ed.; Gilman, A.; Rall, T. W.; Nies, A.S.; Taylor, P. Eds.; Pergamon Press: New York. **1990**, pp. 999-1007.

24. Alvaro, R. F.; Wislocki, P. G.; Miwa, G. T.; Lu, A. Y. *Chem Biol Interact* **1992**, *82*, 21.

25. Chapman, J. D. *New Engl. J. Med.* **1979**, *301*, 1429.

26. Swenson, D. H.; Laster, B. H.; Metzger, R. L. *J. Med. Chem.* **1996**, *39*, 1540.

27. Loetchutinat, C.; Chau, F.; Mankhetkorn, S. *Chem Pharm Bull (Tokyo)* **2003**, *51*, 728.

28. Erickson, J. A.; Jalaie, M.; Robertson, D. H.; Lewis, R. A.; Vieth, M. *J. Med. Chem*. **2004**, *47*, 45.

29. Szczepankiewicz, B. G.; Liu, G.; Jae, H. S.; Tasker, A. S.; Gunawardana, I. W.; von Geldern, T. W.; Gwaltney, S. N.; Wu-Wong, J. R.; Gehrke, L.; Chiou, W. J.; Credo, R. B.; Alder, J. D.; Nukkala, M. A.; Zielinski, N. A.; Jarvis, K.; Mollison, K. W.; Frost, D. J.; Bauch, J. L.; Hui, Y. H.; Claiborne, A. K.; Li, Q.; Rosenberg, S. H. *J. Med. Chem*. **2001**, *44*, 4416.

30. Wu, G.; Robertson, D. H.; Brooks, C. R.; Vieth, M. *J. Comput. Chem.* **2003**, *24*, 1549.

31. Sheldrick, G. M. SHELXTL-97: Program for Crystal Structure Solution and Refinement, University of Göttingen, Göttingen, Germany, **1997**.

32. Chen, X.; Plasencia, C.; Hou, Y.; Neamati, N. *J. Med. Chem*. **2005**, *48*, 1098.

33. (a) WAHBA, A. J.; FRIEDKIN, M. *J. Biol. Chem.* **1962**, *237*, 3794; (b) Davisson, V. J.; Sirawaraporn, W.; Santi, D. V. *J. Biol. Chem.* **1989**, *264*, 9145.

34. Discovery Studio 3.1, Accelrys Software Inc., San Diego, **2011**.

**Table 1.** Crystal structure data for compound **9**.

| Compound | **9** |
|---|---|
| Formula | $C_{14}H_{13}N_5O_3S$ |
| Mr | 331.35 |
| Crystal system | triclinic |
| Space group | *P-1* |
| *a* / Å | 7.380 (2) |
| *b* / Å | 10.208(2) |
| *c* / Å | 11.755(2) |
| $\alpha$ /° | 65.42(3) |
| $\beta$ /° | 81.61(3) |
| $\gamma$ /° | 74.66(3) |
| Volume /Å$^3$ | 776.0(3) |
| *Z* | 2 |
| *Dc*/(g/cm$^3$) | 1.418 |
| $\mu$ /mm$^{-1}$ | 0.231 |
| *F*(000) | 344 |
| Crystal size /mm$^3$ | 0.20×0.10×0.10 |
| *T* /*K* | 293(2) |
| $\theta$ Range /° | 1.91 /25.27 |
| Index range (*h,k,l*) | 0/8,-11/12,-13/14 |
| Reflections collected /unique | 2817 /2181 |
| Data/restraints/parameters | 2181/0/209 |
| Goodness-of-fit on $F^2$ | 1.009 |
| $R_1$, $wR_2$ $[I > 2\sigma(I)]$ [A] | 0.0508/0.1451 |
| $R_1$, $wR_2$ [A] | 0.0691/0.1625 |
| $(\Delta\rho)_{max}$, $(\Delta\rho)_{min}$/(e/Å$^3$) | 0.408/-0.290 |

[A] $R_1 = \Sigma||Fo|-|Fc||/\Sigma|Fo|$, $wR_2 = [\Sigma w(|Fo|-|Fc|)^2/\Sigma w(|Fo|^2]^{1/2}$.

**Table 2.** *In vitro* anticancer activities ($IC_{50}$, $\mu$M) of compounds **9-44** against human tumor cell lines

| Compounds | $IC_{50}$ ($\mu$M) | | |
|---|---|---|---|
| | HepG2[a] | SGC-7901[a] | MCF-7[a] |
| **9** | 17.5 ± 1.2 | 30.1 ± 2.2 | 20.5 ± 1.7 |
| **10** | 5.1 ± 0.3 | 32.3 ± 1.9 | 15.8 ± 1.3 |
| **11** | 2.2 ± 0.2 | 12.5 ± 1.0 | 15.5 ± 0.9 |
| **12** | 10.0 ± 0.6 | 30.5 ± 1.7 | 10.8 ± 0.7 |
| **13** | 5.8 ± 0.5 | 10.2 ± 0.5 | 10.6 ± 0.8 |
| **14** | 4.5 ± 0.7 | 35.1 ± 2.1 | 20.1 ± 1.0 |
| **15** | 6.7 ± 0.7 | 31.7 ± 1.3 | 19.8 ± 0.8 |
| **16** | 9.8 ± 0.3 | 30.3 ± 2.0 | 25.9 ± 2.6 |
| **17** | 1.9 ± 0.4 | 14.1 ± 0.8 | 16.6 ± 1.1 |
| **18** | 0.7 ± 0.2 | 30.0 ± 1.2 | 18.3 ± 1.4 |
| **19** | 4.1 ± 0.4 | 12.2 ± 0.7 | 12.7 ± 0.6 |
| **20** | 3.7 ± 0.3 | 33.7 ± 2.3 | 20.5 ± 2.0 |
| **21** | 0.6 ± 0.2 | 5.3 ± 0.4 | 8.1 ± 0.7 |
| **22** | 15.6 ± 1.4 | 32.6 ± 2.4 | 22.5 ± 1.9 |
| **23** | 7.8 ± 0.9 | 31.9 ± 1.9 | 18.7 ± 1.6 |
| **24** | 19.6 ± 1.5 | 30.5 ± 1.1 | 28.3 ± 1.7 |
| **25** | 4.3 ± 0.4 | 13.8 ± 0.9 | 20.7 ± 1.2 |
| **26** | 4.0 ± 0.3 | 31.1 ± 1.5 | 22.1 ± 1.4 |
| **27** | 11.9 ± 1.1 | 32.8 ± 1.7 | 14.9 ± 1.3 |
| **28** | 8.7 ± 1.6 | 35.9 ± 2.6 | 19.9 ± 1.2 |
| **29** | 16.6 ± 2.8 | 36.7 ± 2.8 | 23.5 ± 1.7 |
| **30** | 11.0 ± 1.2 | 11.7 ± 0.9 | 21.8 ± 1.6 |
| **31** | 10.5 ± 0.9 | 9.6 ± 0.7 | 12.8 ± 0.7 |
| **32** | 14.9 ± 0.8 | 34.8 ± 1.7 | 30.6 ± 2.5 |

| | | | |
|---|---|---|---|
| **33** | 22.6 ± 2.1 | 31.7 ± 2.5 | 29.5 ± 2.2 |
| **34** | 20.5 ± 1.7 | 30.8 ± 1.9 | 25.8 ± 1.9 |
| **35** | 20.2 ± 1.8 | 30.0 ± 1.5 | 39.1 ± 2.6 |
| **36** | 9.6 ± 0.8 | 31.6 ± 2.8 | 28.7 ± 0.9 |
| **37** | 8.4 ± 0.7 | 34.5 ± 2.9 | 29.3 ± 2.1 |
| **38** | 9.4 ± 0.9 | 30.9 ± 1.7 | 26.8 ± 2.4 |
| **39** | 14.8 ± 0.4 | 15.9 ± 0.9 | 12.6 ± 0.8 |
| **40** | 0.9 ± 0.3 | 30.0 ± 1.6 | 20.0 ± 1.2 |
| **41** | 11.6 ± 1.2 | 32.3 ± 1.3 | 40.5 ± 2.7 |
| **42** | 10.6 ± 0.8 | 8.8 ± 1.1 | 30.1 ± 2.3 |
| **43** | 10.1 ± 0.6 | 30.7 ± 2.5 | 34.1 ± 1.7 |
| **44** | 4.1 ± 0.5 | 9.2 ± 1.0 | 14.5 ± 0.6 |
| 5-Fluorouracil[b] | 22.8 ± 1.2 | 28.9 ± 2.2 | 16.7 ± 1.5 |
| Raltitrexed[b] | 1.3 ± 0.2 | 8.7 ± 1.7 | 12.6 ± 2.1 |

[a] Cancer cells were purchased from NanJing KeyGen Biotech Co.,Ltd., which subcultured by State Key Laboratory of Pharmaceutical Biotechnology, Nanjing University; HepG2 (human hepatoma cells), SGC-7901 (human gastric cancer cells), and MCF-7 (human breast cancer cells).

[b] Used as a positive control.

**Table 3.** Inhibitory concentration ($IC_{50}$, $\mu$M) against Isolated human and *E. coli* TS.

| Compds | TS | | ALOGP[c] | Molecualr_weight[c] |
|---|---|---|---|---|
| | Human[a] | *E. coli*[b] | | |
| **11** | 2.1 | >10 | 2.72 | 345.376 |
| **17** | 3.2 | 6.3 | 2.038 | 375.402 |
| **18** | 0.62 | 0.47 | 2.128 | 376.347 |
| **21** | 1.6 | 3.9 | 2.439 | 349.34 |
| **25** | 3.6 | >10 | 3.428 | 373.429 |
| **26** | 3.9 | >10 | 3.634 | 387.456 |

| | | | | |
|---|---|---|---|---|
| **32** | 0.89 | >10 | 2.184 | 421.428 |
| **37** | 1.2 | 1.8 | 0.886 | 348.36 |
| **40** | 0.92 | 1.27 | 1.956 | 347.352 |
| **41** | 2.2 | 4.1 | 2.134 | 366.783 |
| **44** | 1.7 | 2.4 | 2.019 | 389.386 |
| Raltitrexed[d] | 0.38 | 5.7 | 1.528 | 458.488 |
| Pemetrexed[d] | 9.5 | 76 | 1.354 | 426.423 |

[a] Human TS was brought from the Abnova company (http://www.abnova.com/).

[b] *E. coli* strain was kindly supplied by State Key Laboratory of Pharmaceutical Biotechnology, Nanjing University.

[c] The molecular properties had been calculated by the Discovery studio 3.1 suite.

[d] The data has been taken from Ref. 8.

**Table 4.** Antibacterial activity of compounds **18**, **37**, **40** selected in the further study.

| **Compound** | Minimum inhibitory concentrations ($\mu$g/mL) | | | |
|---|---|---|---|---|
| | Gram-negative | | Gram-positive | |
| | *E. coli* ATCC 25922 | *P. aeruginosa* ATCC 27853 | *B. subtilis* ATCC 6538 | *S. aureus* ATCC 530 |
| **18** | 1.56 | 3.13 | 3.13 | 1.56 |
| **37** | 12.5 | 12.5 | 50 | 25 |
| **40** | 3.13 | 6.25 | 50 | 25 |
| Raltitrexed | 25 | 50 | 25 | 50 |
| Kanamycin | 3.13 | 3.13 | 1.56 | 1.56 |

**Table 5.** Experimental, predicted inhibitory activity of compounds **11**, **17**, **18**, **21**, **25**, **26**, **32**, **37**, **40**, **41**, **44,** Raltitrexed, and Pemetrexed against human TS by 3D-QSAR models based on active conformations selected from the previous molecular docking study.

| Compound | TS inhibition | Residual error |
|---|---|---|

| | Actual $pIC_{50}$[b] | Predicted $pIC_{50}$ | |
|---|---|---|---|
| **11** | 5.44 | 5.33 | 0.11 |
| **17** | 5.8 | 5.83 | -0.03 |
| **18** | 6.42 | 6.39 | 0.03 |
| **21** | 5.68 | 5.77 | -0.09 |
| **25** | 5.92 | 5.85 | 0.07 |
| **26**[a] | 6.21 | 6.21 | 0 |
| **32**[a] | 5.49 | 5.39 | 0.1 |
| **37** | 6.04 | 6.12 | -0.08 |
| **40** | 5.66 | 5.63 | 0.03 |
| **41** | 5.02 | 5.17 | -0.15 |
| **44**[a] | 5.41 | 5.57 | -0.16 |
| Raltitrexed[d] | 6.05 | 5.82 | 0.23 |
| Pemetrexed[d] | 5.77 | 6.03 | -0.26 |

[a] Compounds were selected as the test sets while the rest ones were in the training sets

[b] The $IC_{50}$ values of the compounds against TS were converted into $pIC_{50}$ values by using the online calculator. (http://www.sanjeevslab.org/tools-IC50.html)

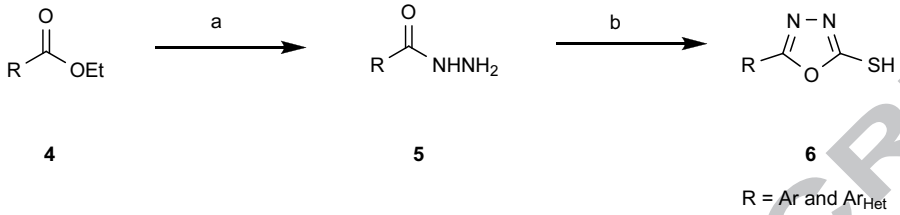


**Scheme 1.** Synthesis of compound **6**. Reagents and conditions: (a) $NH_2NH_2.H_2O$ (85%), ethanol, reflux, 8-12 h; (b) step1. $CS_2$/KOH, ethanol (95%), reflux, 24 h; step 2. HCl, pH = 5~6.

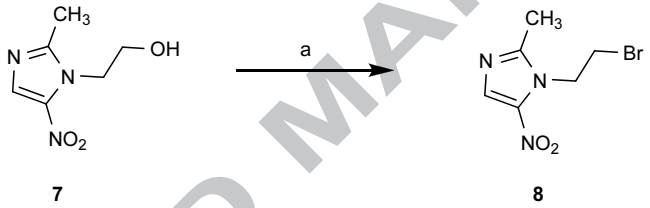


**Scheme 2.** Synthesis of compound **8**. Reagents and conditions: (a) step 1. $Br_2$/$PCl_3$, EtOAc, reflux, 3 h; step 2. NaOH, pH = 5~6.

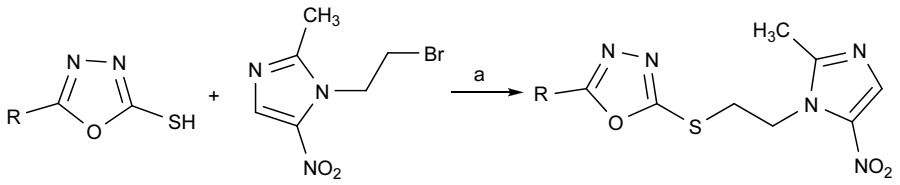


**6** **8** **9-44**

**9:** R= $C_6H_5$-
**10:** R= 2-$CH_3$-$C_6H_4$-
**11:** R= 4-$CH_3$-$C_6H_4$-
**12:** R= 2-$CH_3O$-$C_6H_4$-
**13:** R= 4-$CH_3O$-$C_6H_5$-
**14:** R= 2-$NH_2$-$C_6H_4$-
**15:** R= 4-$NH_2$-$C_6H_4$-
**16:** R= 2-$C_2H_5O$-$C_6H_4$-
**17:** R= 4-$C_2H_5O$-$C_6H_4$-
**18:** R= 2-$NO_2$-$C_6H_4$-
**19:** R= 4-$NO_2$-$C_6H_4$-
**20:** R= 2-F-$C_6H_4$-
**21:** R= 4-F-$C_6H_4$-
**22:** R= 2-Cl-$C_6H_4$-
**23:** R= 4-Cl-$C_6H_4$-
**24:** R= 2-OH-$C_6H_4$-
**25:** R= 4-*i*-Pr-$C_6H_4$-
**26:** R= 4-*t*-Bu-$C_6H_4$-
**27:** R= 4-$(Me)_2N$-$C_6H_4$-
**28:** R= 2-OH-3-$CH_3$-$C_6H_3$-
**29:** R= 2-OH-4-$CH_3$-$C_6H_3$-
**30:** R= 2-OH-4-$CH_3O$-$C_6H_3$-
**31:** R= 3,5-$2CH_3O$-$C_6H_3$-
**32:** R= 3,4,5-$3CH_3O$-$C_6H_2$-

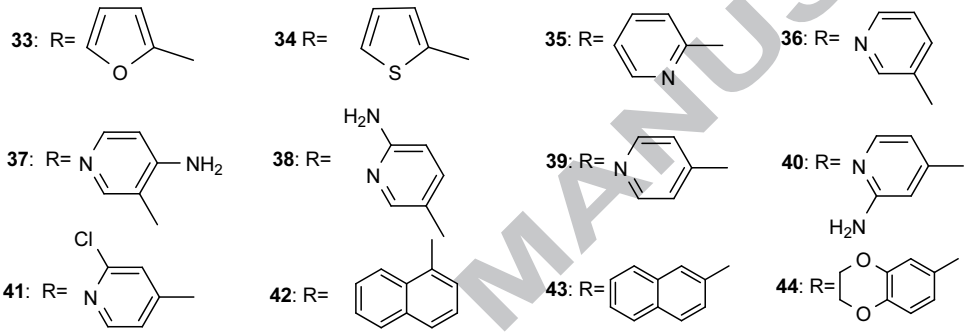


**Scheme 3.** Synthesis of compounds **9-44**. Reagents and conditions: (a) NaOEt, anhydrous ethanol, reflux, 8-36 h.

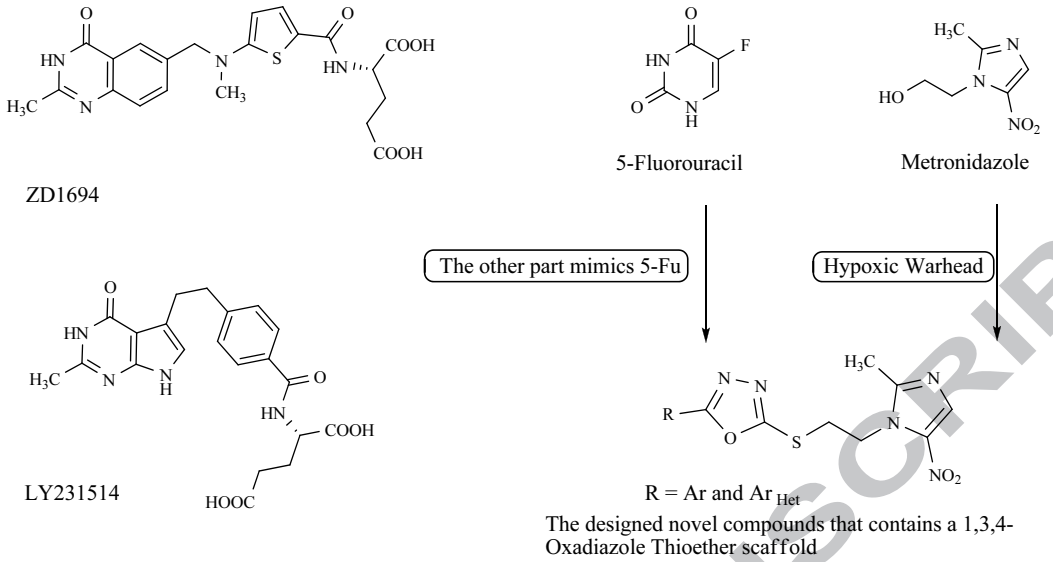


**Figure 1.** The three known thymidylate synthase (TS) inhibitors: Raltitrexed (ZD1694), Pemetrexed (LY231514), and 5-Fluorouracil (5-FU) presented above; meanwhile, based on the 1,3,4-oxadiazole skeleton, a series of new TS inhibitors that could be divided into the two parts have been designed. It is apparent that one of the two fragments is the 1,3,4-oxadiazole structure that belongs to its pharmacophore and could mimic the function of 5-FU, and the other is composed of the metronidazole moiety that is a good warhead directing to the hypoxic tissue of most tumors.

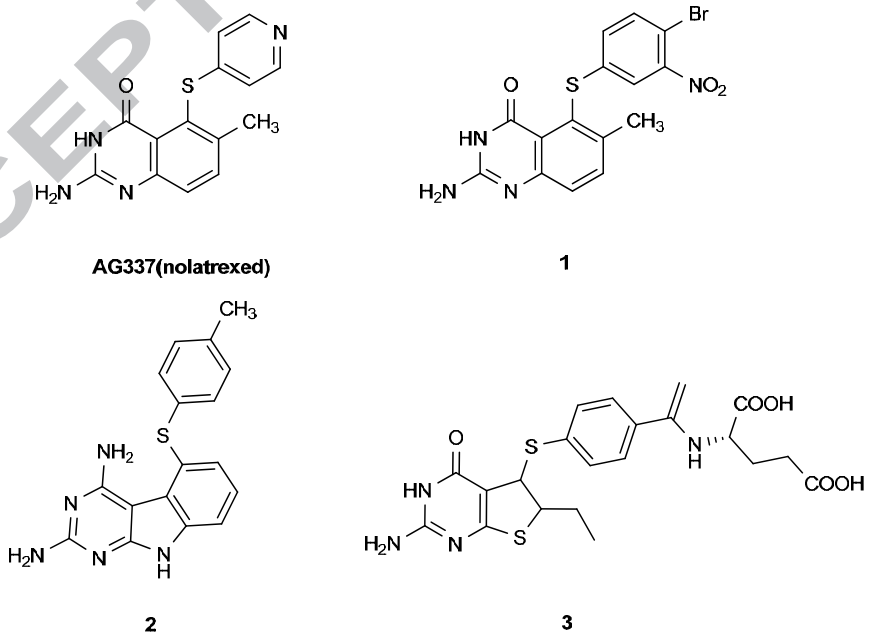

**Figure 2.** Several designed thymidylate synthase (TS) inhibitors in the past ten years. Moreover, the three compounds **1**[10], **2**[11], and **3**[12] had been developed by the same research group.

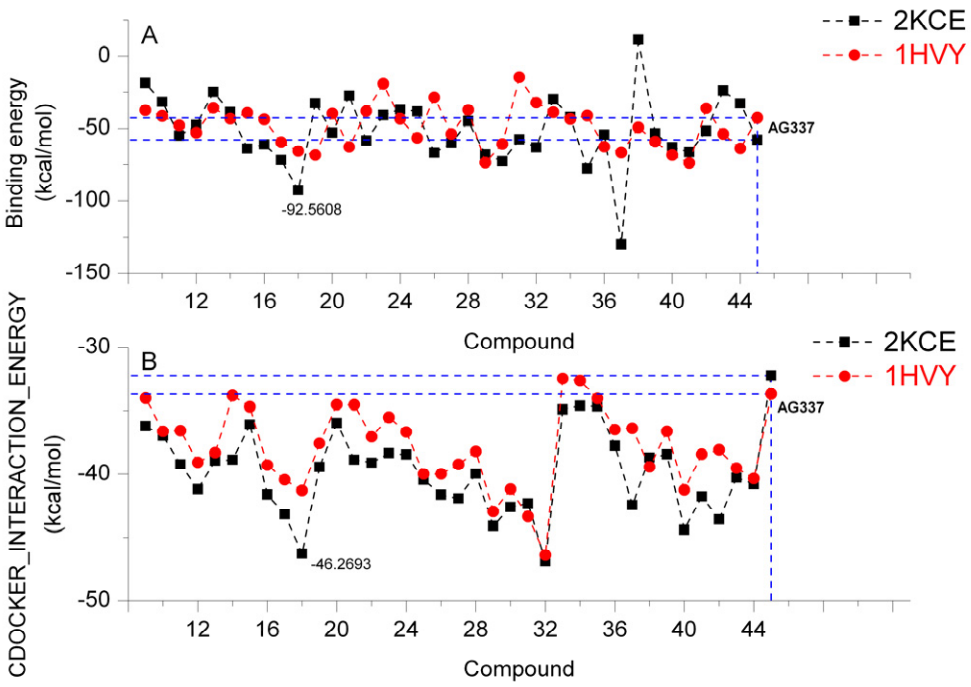


**Figure 3.** The binding energy and CDOCKER_INTERACRION_ENERGY between the designed compounds and two kinds of thymidylate synthases in the protein database bank (http://www.rcsb.org/, PDB code: 1HVY derived from human TS and 2KCE derived from *E. coli* TS) is calculated by the Discovery studio 3.1 suite. A) The binding energy; B) The CDOCKER_INTERACRION_ENERGY. Compared with the positive drug, AG337, most of the small molecules below the blue dash lines would possess lower binding energy and interaction energy and be likely to exhibit more potent against both of the two protein targets.

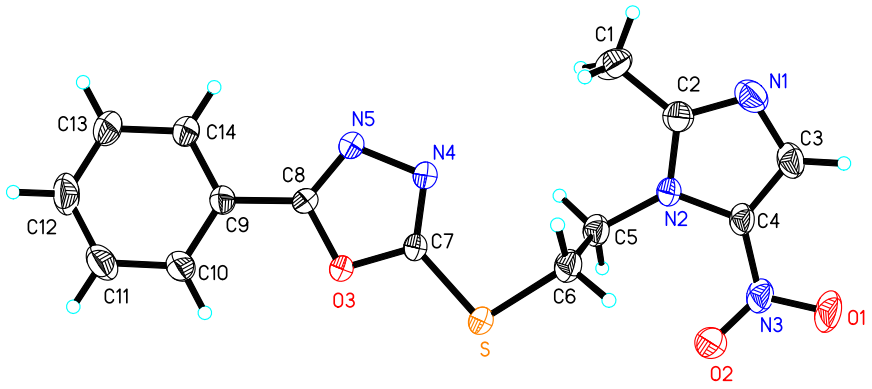


**Figure 4.** Molecular structure of compound **9**. Displacement ellipsoids are drawn at the 30% probability level.

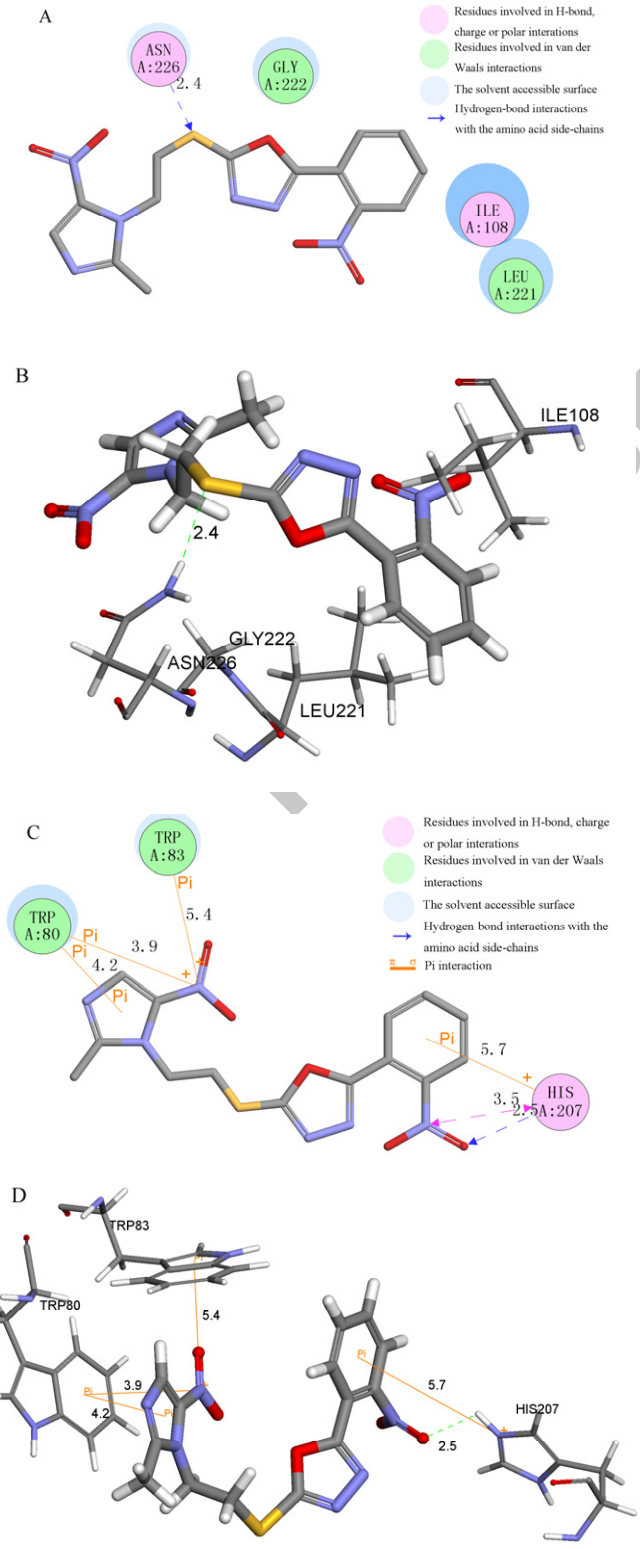


**Figure 5.** The two kinds of binding modes between the active conformation of

compound **18** and two TS proteins (PDB code: 1HVY and 2KCE) provided by the CDOCKER protocol (Discovery Studio 3.1, Accelrys, Co. Ltd). A) The 2D diagram located at the human TS binding pocket (1HVY) displayed the interaction between **18** and the targeted protein, in which a hydrogen bond (2.4 Å) has been depicted. B) The corresponding stereoview of the interaction mode between **18** and the 1HVY TS protein. C) The 2D diagram located at the *E. coli* TS binding pocket (2KCE) displayed the interaction between **18** and the targeted protein, in which four kinds of interactions have been presented: three *Pi-Cation* bonds (yellow), one *Pi-Pi* bond (yellow), one hydrogen bond (yellow) and one charge interaction (pink) formed between **18** and three amino acids (Trp80, Trp83, His207) in the substrate binding pocket. D) The corresponding stereoview of the interaction mode between **18** and the 2KCE TS protein.

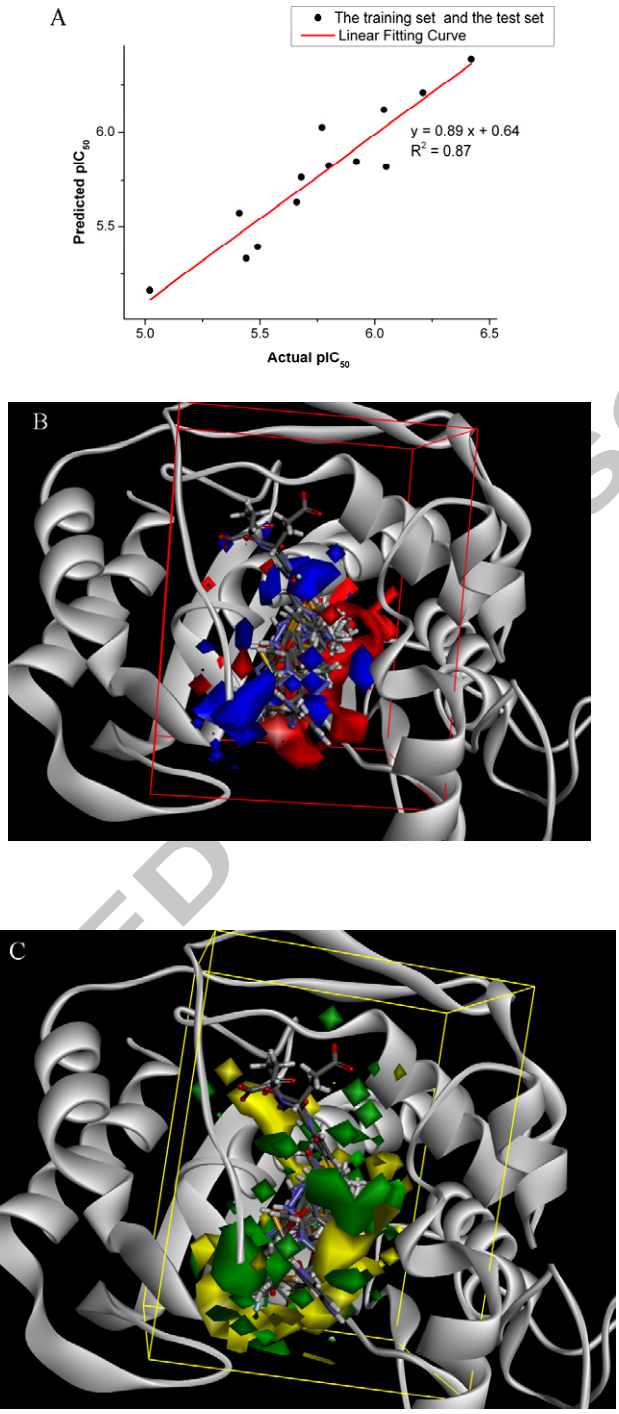


**Figure 6.** A) The predicted versus experimental $pIC_{50}$ value for the inhibition of TS. B) Isosurface of the 3D-QSAR model coefficients on electrostatic potential grids. The blue triangle mesh represents positive electrostatic potential and the red area represents negative electrostatic potential. C) Isosurface of the 3D-QSAR model

coefficients on Van der Waals grids. The green triangle mesh representation indicates positive coefficients; the yellow triangle mesh indicates negative coefficients.

# Novel 1,3,4-Oxadiazole Thioether Derivatives Targeting Thymidylate Synthase as Dual Anticancer/Antimicrobial Agents

*Qian-Ru Du [a+], Dong-Dong Li [a+], Ya-Zhou Pi [a], Jing-Ran Li [a], Jian Sun [a], Fei Fang [a], Hai-Bin Gong [b,*], Hai-Liang Zhu [a,*]*

[a] *State Key Laboratory of Pharmaceutical Biotechnology, Nanjing University, Nanjing 210093, P. R. China.*

[b] *Xuzhou Central Hospital, Xuzhou 221009, P. R. China.*

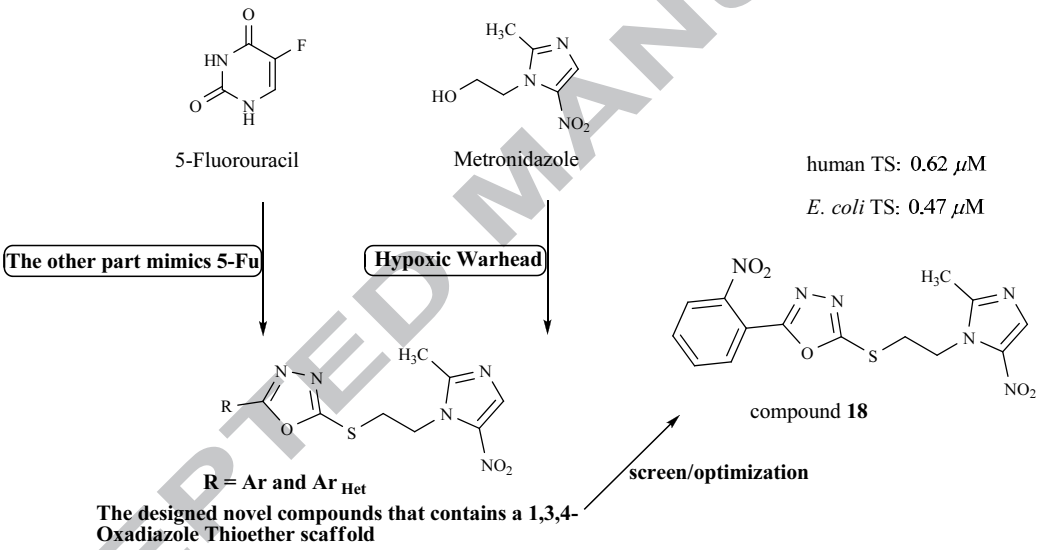


**Abstract:** A series of novel 1,3,4-oxadiazole thioether derivatives (compounds **9-44**) were designed and synthesized as potential inhibitors of thymidylate synthase (TS) and as anticancer agents. The *in vitro* anticancer activities of these compounds were evaluated against three cancer cell lines by the MTT method. Among all the designed compounds, compound **18** bearing a nitro substituent exhibited more potent in vitro anticancer activities with $IC_{50}$ values of 0.7 ± 0.2 $\mu$M, 30.0 ± 1.2 $\mu$M, 18.3 ± 1.4 $\mu$M, respectively, which was superior to the positive control. In the further study, it was identified as the most potent inhibitor against two kinds of TS protein (for

human TS and *E. coli* TS, $IC_{50}$ values: 0.62 $\mu$M and 0.47 $\mu$M, respectively) in the TS inhibition assay *in vitro* and the most potent antibacterial agents with MIC (minimum inhibitory concentrations) of 1.56-3.13 $\mu$g/mL against the tested four bacterial strains. Molecular docking and 3D-QSAR study supported that compound **18** can be selected as dual antitumor/antibacterial candidate in the future study.